# THE SYSTEM IRON-TIN

by

John H. Wood.

A Thesis Presented To The Committee On
Graduate Studies, University Of Manitoba,
In Partial Fulfillment Of The Requirements
For The Degree Of Master Of Science.

April 1948.

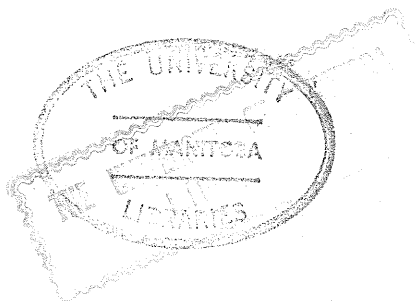

TO DR. A. N. CAMPBELL

In grateful appreciation for
his unfailing interest and
constant guidance.

## ACKNOWLEDGEMENTS

The author wishes to express his appreciation to the Consolidated Mining and Smelting Company Limited, of Trail, B.C., for their generous Fellowship Grant to the author, and for their extra grant for the purchase of special equipment.

To Mr. Bruce C. Lutz, formerly a Lecturer in the Department of Physics, the author expresses his sincere thanks for the design of the electronic control circuit used in this investigation. Without this, the method of investigation used would probably have proved to be impossible.

The author must also acknowledge the frequent advice and assistance of Mr. Robert Bird, University Technician, and his assistant, Mr. Gordon Trider, in the construction and maintenance of the equipment used.

# THE SYSTEM IRON-TIN

## INDEX

# INTRODUCTION

# THE SYSTEM IRON-TIN

## INTRODUCTION

Although many intermetallic compounds of iron and tin had been claimed prior to 1907, it was not until that year, with the publication by Isaac and Tammann of a paper "On the Alloys of Iron with Tin and Gold"[1], that a constitutional diagram was formulated. Since then many modifications have been made as other workers have sought to improve the accuracy of the studies (See Section on Previous Investigations).

The main interest in this system has been its application in the tin-plating industry, for which many thorough studies of the mechanism of tin-plating, e.g. Jones and Hoare[2], have been made. During the recent war the steel mills became more interested in this system in view of the large amount of tinned steel being returned to the mill as scrap[3]. As a result, it became necessary to know how much tin could be tolerated in the charges fed to the scrap furnaces, and how such charges should be handled.

However, this investigation arose from neither of the above considerations. At Kimberley, B.C., the Consolidated Mining & Smelting Company Ltd. operate an electric tin smelting plant.[4] The tin concentrate recovered from the tailings of the Sullivan concentrator

is charged to a 400 k.v.a. 3 phase electric furnace, along with the necessary coke and lime, for smelting, the slag being skimmed at about 2200° F. (ca. 1200° C.). The crude tin is tapped at about 1900°-2100° F. (ca. 1040°-1160° C.), and run to a #1 pot, and held there until its temperature drops to 700° F. (ca. 370° C.). After drossing, it is pumped to another pot, #2, from where it is pumped, at as low a temperature as possible, through a unique filter of Consolidated design. The filtrate goes to a further pot, #3, which feeds the casting rack.

Thus, to quote from Jones and Thunaes[4], "The Trail method takes full advantage of the law of iron solubility in tin..... Iron is quite soluble in tin at high temperatures but, on lowering the temperature to near the melting point of tin, iron separates as a solid component, $FeSn_2$ (containing about 19 per cent Fe) suspended in practically Fe-free tin. Hence, by application of filtering methods, the solid $FeSn_2$ is separated from the liquid tin, and the iron content of the crude tin is lowered to 0.006 per cent. In practice, the iron content of the tin is considerably lower for temperatures up to 800° F. (ca. 430° C.) than shown by published Sn-Fe diagrams. This would seem to indicate that the published diagrams are in error in the area approaching pure tin.....

"The average assay of refined tin is :

| | | | |
|---|---|---|---|
| Fe | 0.006% | Al | 0.005% |
| Pb | 0.31 | Mn | 0.005 |
| Cu | 0.006 | Co | 0.004 |
| Zn | 0.005 | Sb | 0.01 |
| Bi | 0.002 | Sn | 99.647 " |

C. H. Wright,[5] in discussing this, wrote "This low iron content of tin filtered at the above temperature (about 353°C.) led to a series of investigations in which filtering temperature was varied between 250°C. and 500°C. In the course of our experiments, we in no case obtained a filtrate containing more than 0.02% iron, and at temperatures below 400°C. the filtrate in no case contained more than 0.01% iron."

In another letter[6] the results of some other work were given. Some tim was filtered at 560°F. (300°C.) to give a filtrate of 0.01% iron. This was reduced to 0.002% by a subsequent filtration.

In view of the above evidence that the literature values for the solubility of the iron compounds in tin were considerably too high, a further investigation of the system, especially for low Fe content, was considered desirable.

# THEORETICAL CONSIDERATIONS

# THEORETICAL CONSIDERATIONS

## I. Introduction:

An alloy is a mixture and/or solution in a metal of one or more other metals or non-metals. These materials exhibit physical and chemical properties which are different from those of the constituent elements.

Prior to the enunciation of the Phase Rule, many isolated experimental investigations on metallic systems had been conducted, but it had been found impossible to correlate these fragments. Although Willard Gibbs[7] first presented his theory of phases in 1876, it was not until the end of the century that Jüptner[8] and Le Chatelier[9] suggested its application to alloys. In the meantime, Bakhius Roozeboom[10] had published a series of papers deriving all possible equilibrium diagrams from the Thermodynamic Potential $\phi$. Using the symbols of Lewis & Randall[11] this function is now identified with the Free Energy F. For equilibrium F must be a minimum where

$$F = E - TS + PV \quad \text{.....(1)}$$

F = Free Energy
E = Internal Energy
T = the absolute temperature
S = entropy
P = pressure
V = volume.

It is interesting to note that, even though the principles of phase equilibrium were clearly enunciated almost fifty years ago, Lipson & Wilson[12] point out that there are still many published equilibrium diagrams which contain details which are theoretically impossible.

## II. The Freezing Point Depression and Composition:

Following the enunciation by Raoult of his Law of Freezing Point Depression, viz. the lowering of the freezing point of a solution is proportional to the concentration of the dissolved solute, van't Hoff introduced his Theory of Solutions which assumed that the dissolved body is in a state analogous to that of a perfect gas. Using the van't Hoff concept, it may be easily shown that, to a first approximation [13], when pure crystalline solvent separates as the solid phase,

$$\triangle T_f = \frac{RT_o^2 M_1 m}{1000\, L_f} \qquad \ldots\ldots\ldots\ldots\ldots (2)$$

where $\triangle T_f$ is the Freezing Point Depression
$R$ is the Gas Constant
$T_o$ is the Freezing Point of the pure solvent
$M_1$ is the molecular weight of the solvent
$m$ is the molality of the dissolved solute
$L_f$ is the Molar Latent Heat of Fusion of the solvent.

From 1890 to 1895, Heycock & Neville studied the lowering of the freezing points of mercury, cadmium, bismuth, lead, and tin, when alloyed with other metals. They showed[14] the freezing point depressions were consistent with the above equation, and that the molecular weights of the dissolved solutes, for almost all metals studied, correspond to the atomic weights of the dissolved metals. This is only valid for small to moderate quantities of solute in molten alloys. Thus, in reverse,

assuming that any solute metal is present in the monatomic state, and knowing the freezing point depression, the concentration of dissolved solute may readily be calculated by equation 2.

In considering any solutions, the freezing point is defined as the first temperature point at which the solution is in equilibrium with the stable solid phase. It must automatically follow that for equilibrium the vapour pressures of the solid and liquid phases are identical. Strictly, when two phases are in equilibrium, the fugacity of the substance in both phases[15], rather than the vapour pressure, is the same. However, the discussion here, of the three possible cases that arise, will use vapour pressures.

First, in Fig. 1, if AB is the vapour pressure curve of pure liquid, and BC of crystalline solvent, then B, their point of intersection, must correspond to the freezing point of pure liquid, $T_o$. Since the addition of a solute lowers the vapour pressure of a solution, e.g., curve DE of Fig. 1, it must follow, when crystalline solvent separates out, it is in equilibrium at a lower temperature than $T_o$ since DE intersects BC at E, which corresponds to $T'$, a lower temperature than $T_o$. The exact amount of lowering is given by equation 2. As solvent freezes out, the solution becomes richer in

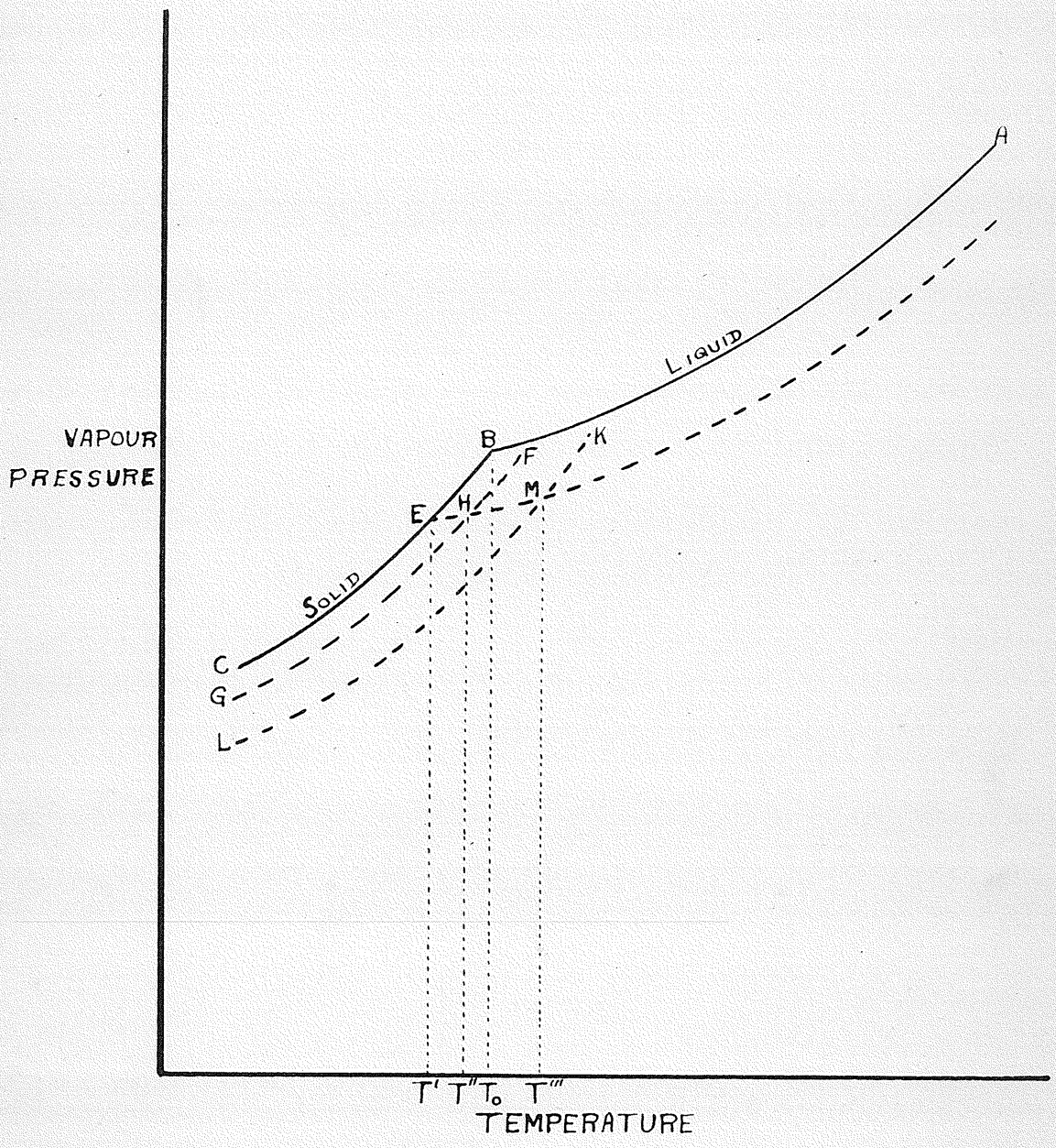
VAPOUR
PRESSURE
A
LIQUID
B
K
F
M
E
H
SOLID
C
G
L
T' T'' T₀ T'''
TEMPERATURE

FIGURE 1

solute, and hence the freezing point is continually lowered until the eutectic is reached and complete solidification occurs. The equilibrium diagram for this case will then correspond to Fig.2(a). Here there is a eutectic with no solid solution present.

If, however, instead of having pure solvent as the solid phase, there is crystalline solvent containing some solute (less than is present in the original solution), the vapour pressure of the solid phase is lowered, GHF on Fig.1. Now the first solid phase will appear when point H is reached. This corresponds to a temperature $T''$ which is higher than $T'$. Since, as solidification occurs, the solution becomes still richer in solute, the freezing point is continually lowered as in the previous case. However, the amount of depression must always be less than in the preceding case. The corresponding equilibrium diagram is shown in Fig.2(b).

In all cases where a eutectic is formed, the application of equation 2 will give the eutectic composition, provided the concentration of solute is small enough that the Ideal Gas Law conditions are met. The value of $\triangle T_f$ is the difference in temperature between the freezing point of the pure solvent and that final freezing point obtained when solute is dissolved in the pure solvent. Thus, assuming the results of Heycock &

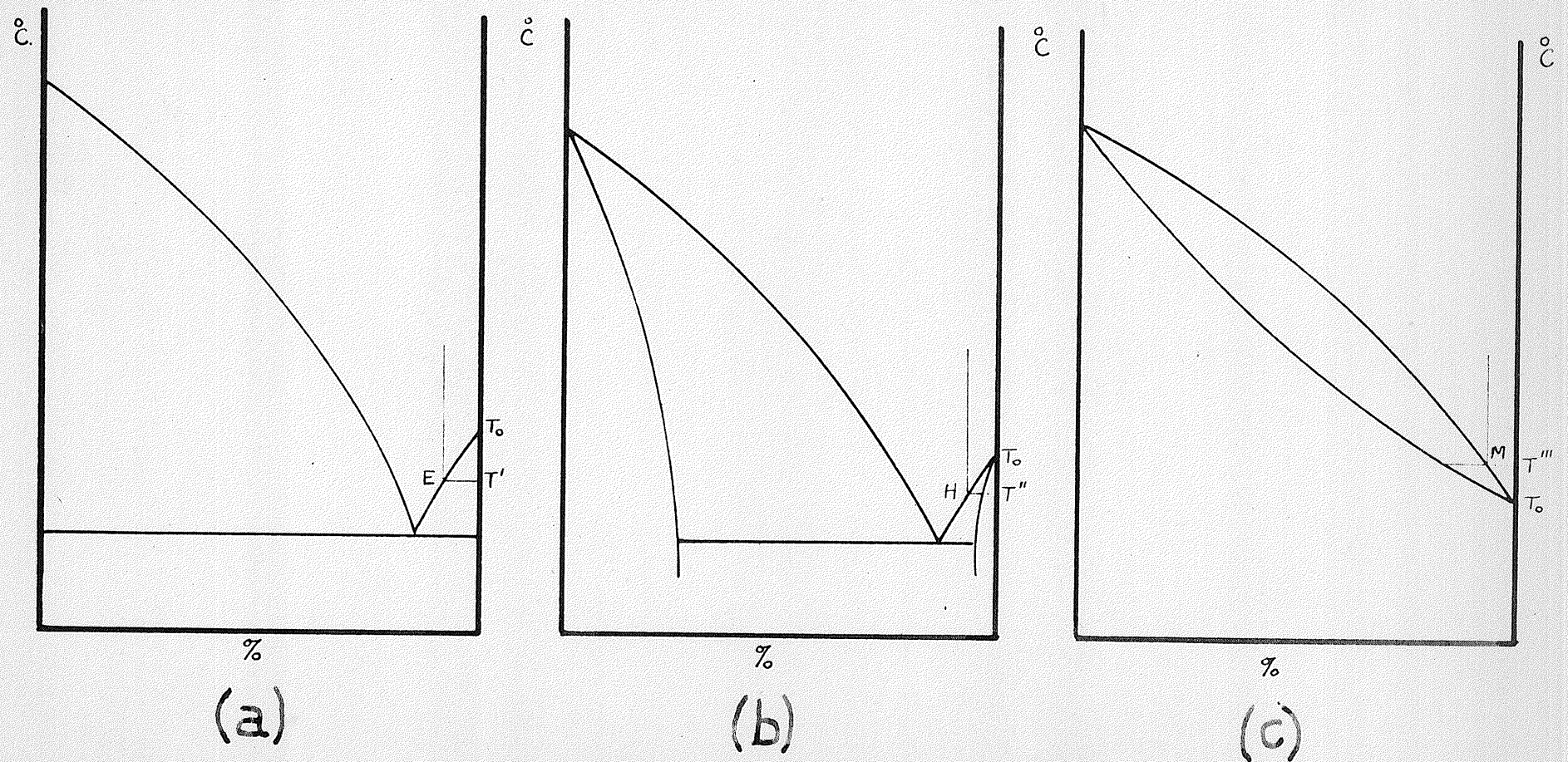


FIGURE 2

Neville's work, namely, that the solute is present in the monatomic state, the composition of the eutectic is obtainable by direct calculation.

A third case arises. If the solid phase formed contains more solute than the initial solution, the vapour pressure of the solid phase is lowered even more than before, to KL. Now, solidification occurs initially at M or $T'''$, a temperature higher than $T_o$, the freezing point of pure solvent. As solidification proceeds, the solution becomes poorer in solute, and the solid richer, so the freezing point continues to rise with composition. Hence, we have the equilibrium diagram of Fig.2(c), namely solid solution formation with freezing point elevation.

In theory, the first case may be considered as a special case of the second, as no solid solution occurs. Another special case is the transition between the eutectic formation and solid solution. Heydock & Neville[16] claimed to have found a system where the solid and liquid had the same composition, and hence the freezing point was constant. This case is very much to be doubted, indicating rather the closeness of approach to the transition between the extremes.

For more concentrated solutions, many new factors[16] become important which invalidate many of the assumptions made in the derivation of equation 2. As a result, the theoretical treatment, and the resultant equations, become very complicated.

## III. Methods of Determining Equilibrium Diagrams.

Any internal change in the physical or chemical nature of a substance usually alters many of its physical properties, as, for example, its magnetic and thermoelectric behaviour, electric resistance, specific heat, dimensions, density, and microscopic structure[17].

### A. Thermal Analysis:

All methods of thermal analysis assume that chemical and physical transformations within a substance are accompanied by a heat effect. Thus any time a heat effect is observed, it must correspond to a transition from one stable phase or component to another. Some very complete discussions of the methods of thermal analysis have been published[17,18]. A summary of the main methods, with some of their advantages and disadvantages, is given here. All these methods give a "break" in the plotted results when a transformation, either solid to solid or liquid to solid, occurs.

#### 1. Temperature - Time Curves:

(a) $\theta$ vs t - The variation of temperature with time is the simplest possible curve. It cannot distinguish between phenomena proper to the substance studied and those due to outside conditions.

As originally used by Frankenheim[19], the sample was "free cooled". Plato[20] introduced linear cooling

to accentuate any observed heat effects. This, on plotting, yields results as shown in Fig.3(a).

(b) $\theta$ vs t, $\theta'$ vs t (or $\theta$ vs $\theta'$) - Here $\theta$ is the temperature of the sample and $\theta'$ that of the furnace. If alternate readings are taken of $\theta$ and $\theta'$, and plotted against time, a curve as in Fig.3(a) is obtained. The Temperature-Time curves are very readily adaptable to automatic control and recording

2. Differential Curves:

(a) $\theta$ vs t, $\theta-\theta'$ vs t - Here, alternate (or simultaneous) readings of the temperature of the sample, and of the difference in temperature between the sample and a neutral body[21], are taken, giving a plot as shown in Fig.3(b). The neutral body is a body of the same heat content as the sample being studied, and is so situated in the furnace that sample and neutral body are at the same temperature initially and cool at the same rate until a transformation occurs. Of course, the neutral body must undergo no transformation involving a heat effect within the temperature range studied.

This method, introduced by Roberts-Austen, yields the maximum in sensitivity and offers no limitation as to the temperature range of applicability.

However, in practice, it is impossible to maintain $\theta-\theta'$ constant. This is due to the difference in mass,

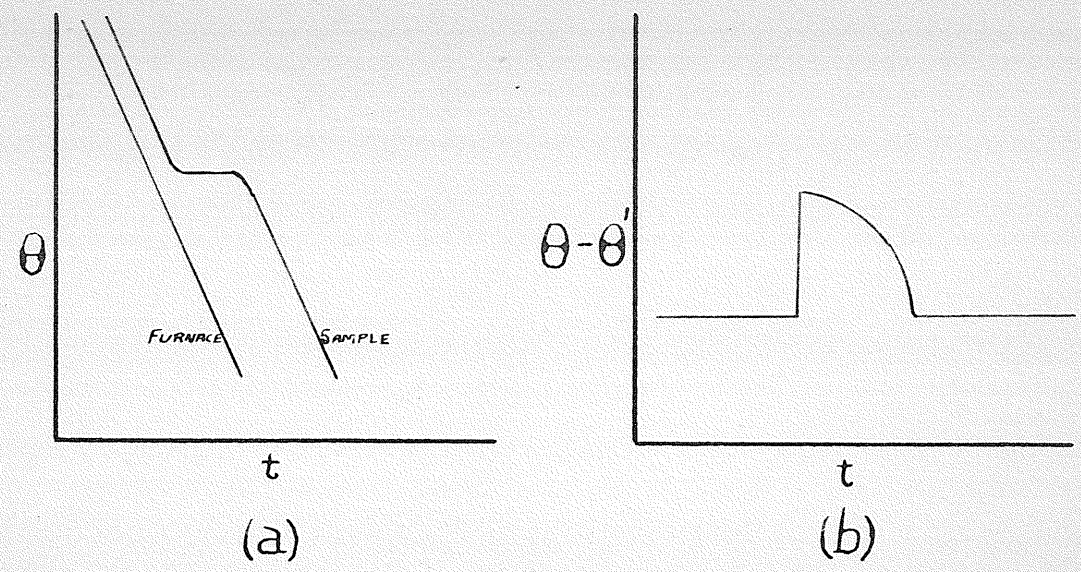


(a)




(b)

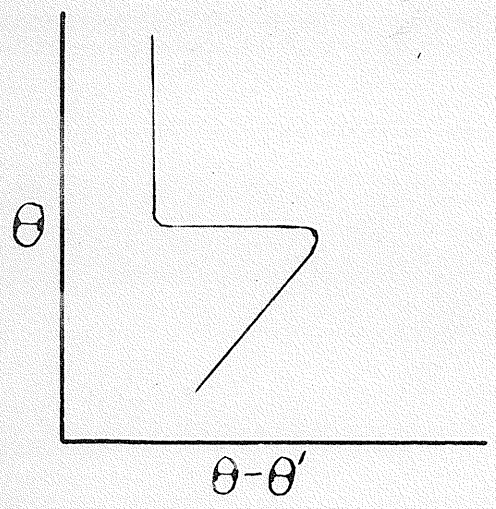


(c)

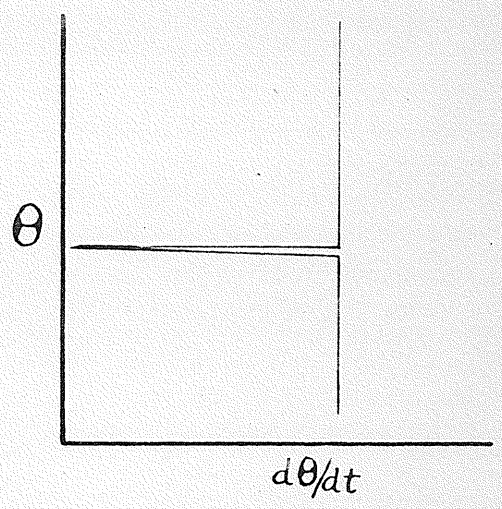


(d)

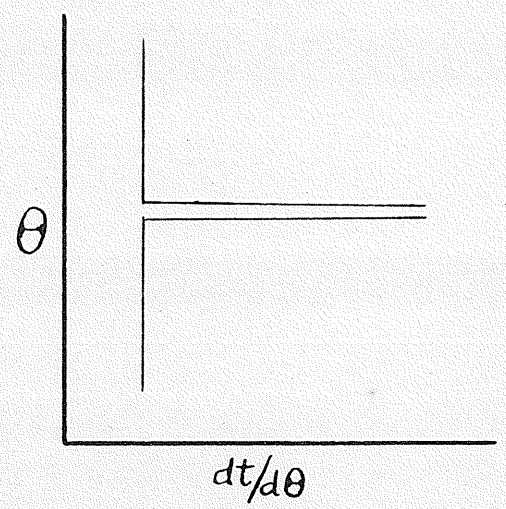


(e)

FIGURE 3

specific heat, conductivity, emissitivity, as well as the relative heat capacities of furnace and the enclosed samples. The above considerations result, in practice, in a somewhat distorted curve.

(b) $\theta$ vs $\theta-\theta'$ - Saladin[22] took the results from the above method and replotted, removing the time variable from the considerations, (Fig.3(c)). The method cannot be adapted to recording instruments, and has little to commend it except for the compactness of the results.

(c) $\theta$ vs $\frac{\theta-\theta'}{\triangle\theta}$ - This "Derived Differential" curve was suggested by Rosenhain[18] to eliminate some of the difficulty in interpreting data of the Roberts-Austin method, the plot of which is distorted because of the reasons already mentioned. As it expresses $\theta$ in terms of the difference $\theta-\theta'$ for the same temperature increments, the distortion is reduced somewhat. Many workers consider this the most valuable plot for extreme sensitivity. The plotting is, obviously, quite laborious.

3. Direct and Inverse Rates:

(a) $\theta$ vs $\frac{d\theta}{dt}$ - This plot, Fig.3(d), allows the measuring of the speed of a transformation. However, since no neutral body is used, the effects of the heating

or cooling of the system cannot be compensated.

(b) $\theta$ vs $dt/d\theta$ - This, also, is used for determining rates of transformation. (Fig.3(e).)

Thermal analysis allows the calculation of the composition of the constituent solid phases, as these correspond to the compositions for the maximum duration of the transition.

B. Isothermal Analysis:

As the name implies, this method involves the bringing of a system into equilibrium at the temperature desired for investigation, and then determining the desired information, usually the composition of the liquidus.

The system of annealing, as practiced for microscopic and X-ray studies, is really isothermal analysis, since the equilibrium is "frozen" by quenching the sample. This will be discussed later under separate headings.

The method of isothermal analysis is classical in the investigation of systems involving salts and water. The method has not been widely used, however, in the study of alloys. Nevertheless, the principle is still the same since the liquidus curve is actually the solubility curve.

Although the method of quenching from determined temperatures had been employed by Howe[23] in 1893, it was not used on non-ferous systems until the investigation of the Cu-Sn system by Heycock & Neville[24] in 1902.

H.J. Miller[25] further investigated this system isothermally, and determined a few points on the liquidus for the high tin end of the diagram. Parts of the liquidus of Al-Ti[26] and Ni-Sn[27], and the miscibility gap of the system Zn-Pb[28], have also been obtained by this method.

The obvious difficulty lies in obtaining a suitable sample of the liquid present without contamination from the excess solid phase. It follows that if the density of the liquid and solid are close, the method may become useless, since the separation becomes too difficult to effect.

C. Microscopic Analysis:

In 1665, Robert Hooke "described the appearance of lead crystallizing from its alloy with silver, and further described and drew the magnified surface of a polished steel razor blade", (Desch)[29]

Modern methods are more systematic in nature. An alloy of the desired constitution is annealed at the

at the temperature to be investigated. After annealing, it is quenched as rapidly as possible (usually within less than half a second). A section is then polished and etched with a suitable reagent. This etching reagent attacks the various constituents of an alloy differently, thus giving a crystal relief suitable for microscopic examination. Sometimes, for very soft metals, it is necessary to remove the flowed surface obtained during grinding before the final etching is performed. Heat etching or electrolytic etching are alternatives to chemical etching.

By studying alloys of the same composition quenched from different annealing temperatures, it is possible to recognize the constituents common to a given phase region. Thus a series of determination may set, quite closely, the various phase boundaries. Since, in general, this method involves macro samples, the period of annealing may be of considerable length.

The main point of criticism, especially if the work is not being done simultaneously by another method, is ensuring that no segregation has occurred during quenching, and that the quenched sample does truly represent the conditions of the annealing temperature and not those of some lower temperature due to a very rapid transition, the original quenched state being too metastable. To circumvent this difficulty, work has been done on both

high and low temperature etching and microscopy[30], but the methods become more difficult.

Obviously, the microscopic method cannot identify and give the constitution of unknown constituents. Hence, it must be used only in conjunction with other methods.

D. X-ray Analysis:

The theory of X-ray analysis has no part in this work; reference should be made to one of the many standard text-books on the subject[31,32,33]. It is sufficient to say that the scattering pattern of X-rays from crystals is dependent on the nature of the constituent atoms of a crystal and upon their spacial arrangement, and thus positive recognition can be accorded to every different crystal. Analytical mathematical methods readily allow the calculation of the crystal lattice parameters, and hence allow the determination of the atomic ratio of the constituent elements, i.e. the "formulae" of the solid phases.

Arne I. Westgren[34] has cited some of the many advantages of the application of the X-ray method to the study of alloys. "The investigation is able to give full evidence regarding the number of phases that occur in an alloy system..... Further, their composition may generally also be found out in this

manner, and many cases determined with a very high degree of accuracy..... The X-ray interferences give evidence regarding the crystal structure of the different alloy phases, and this provides a certain insight into their chemical characteristics which the earlier metallographic methods could do but incompletely. Certain laws governing the coupling of metal atoms into combined phases have been traced thereby, and the structural analogies have been proved to exist between different alloy systems. The intermetallic reaction products are not formed so capriciously as believed earlier, but instead, in many cases, a certain simpler relation seems to exist between crystal structures and the properties of the constituent atoms....."

In the investigation of the ternary systems, the X-ray powder photographs are of even greater value in quickly mapping out the diagram(35).

Like the microscopic method, the X-ray method normally uses quenched annealed samples, and accordingly the same difficulty of determining whether transformations have occurred during quenching arises. However, the danger is not so great here since the sample is annealed in the form of fine filings which can be quenched far more quickly and effectively than massive pieces suitable for microscopic study.

These filings must be made from the homogeneous alloy

and must be so made as to avoid contamination, sometimes being made out of contact with air.

To remove the uncertainties of quenching, and at the same time to investigate alloy phenomena at high temperatures, methods of X-ray study up to 1000°C. have been developed(36). The most difficult part of the procedure is then the determination of the temperature of the small samples being investigated.

Since the X-ray method provides one photograph showing the number of phases present, the lattice spacing of each phase (and hence usually the composition of the phase), and the relative amounts of the phases, this method has now become perhaps the most important method for modern metallographic research.

E. Other Physical Properties:

The use of physical properties to study discontinuities in alloys was pioneered by Matthiessen(37) (1863 on), thirty years before equilibrium diagrams were first suggested.

Many of the physical properties not already mentioned are valuable for certain special cases where the previous methods are not suitable, or where it is desired to obtain further information to confirm results obtained.

Since most changes in the solid state are accompanied by a change in volume, this method becomes a valuable tool. One method is essentially that of the classical

dilatometer work of van't Hoff[38], the sample being maintained at each temperature investigated until equilibrium is established. When a transformation line (phase boundary) is crossed, there is a sudden break in the volume-temperature curve corresponding to this. In general, the method is adapted to the system being investigated.

In the event of liquid metals and alloys in the low temperature ranges, direct density determinations are possible. For high temperature ranges, the use of a sinker suspended from a balance has proven practical for density measurements of liquids for temperatures as high as liquid iron[39].

Other physical properties of varying usefulness, but which show the same "breaks" at phase boundaries, are hardness, electrical conductivity, thermo-electric power, magnetic properties, colour, and electrolytic potential.

# PREVIOUS INVESTIGATIONS

## PREVIOUS INVESTIGATIONS

### I. The Pure Components:

#### A. Tin:

Various values have been suggested for the melting and/or freezing point of tin. In 1911 Waidner & Burgess[40] found the melting point to be 231.86°C. Adams & Johnston[41] in 1912 reported the freezing point of Sn on two trials as 231.733° and 231.88°C. In 1917 Holborn & Henning[42] set the value at 231.83°C.

Tin undergoes two polymorphic transitions as shown by the equation

$$\alpha \text{ Tin} \overset{18^\circ}{\rightleftharpoons} \beta \text{ Tin} \overset{170^\circ}{\rightleftharpoons} \gamma \text{ Tin}$$

| | $\alpha$ Tin | $\beta$ Tin | $\gamma$ Tin |
|---|---|---|---|
| Colour | Grey | White | White |
| Crystal Form | Cubic | Tetragonal | Rhombic |

#### B. Iron:

In 1930 Jenkins & Gayler[33] found the melting point of iron to be 1527 ± 3°C. Previously, the accepted value had been about 1525°C. However, in 1940 it was shown that for iron free of oxygen the melting point was 1535°, and when saturated with oxygen 1524°C.[44]

Iron undergoes several transitions upon heating. The temperatures of these transitions have been the subject of considerable investigation.

The first change $\alpha$-ferrite $\rightleftharpoons$ $\beta$-ferrite at 760° is not now considered a polymorphic change. It corresponds to the loss of ferro-magnetic properties.

It is a progressive change, and does not take place at a definite temperature.

Thus, for phase changes, there remain

$$\alpha\text{-ferrite} \underset{\rightleftharpoons}{\overset{910^{\circ}}{\rightleftharpoons}} \gamma\text{-ferrite} \underset{\rightleftharpoons}{\overset{1400^{\circ}}{\rightleftharpoons}} \delta\text{-ferrite}$$

$\alpha$-ferrite and $\delta$-ferrite are the same, and in a binary alloy the $\gamma$-form corresponds to a loop near the 100% iron. There is considerable hysteresis in the $\alpha - \gamma$ transition depending on whether it is determined as a heating or cooling change. One of the more recent works[45] gives the $\alpha \rightarrow \gamma$ as $910.5^{\circ} \pm .6^{\circ}$C. and the $\gamma \rightarrow \alpha$ as 2 to $2\text{-}1/2^{\circ}$ lower.

## II. The Preparation and Properties of Certain Intermetallic Fe-Sn Compounds:

In 1830 Lassaigne[46] obtained from an iron distilling retort for tin a specular residue which he claimed had a composition corresponding to $Fe_3Sn$. During the next seventy years, various workers obtained, through devious means, many Fe-Sn materials for which they claimed empirical formulae. In 1905 Stevanovic[63] cast considerable doubt upon the chemical entity of many of the alleged compounds. Indeed, many of these, including even some recent references, have not been proposed in any diagram to date.

Table I gives a list of all known reported intermetallic compounds of Fe and Sn. Those recognized on the basis of the most recent work are especially noted.

Table I - Fe-Sn Intermetallic Compounds

| Formula | Claimant | Date | Reference No. | Recognized by Ehret & Gurinsky | Remarks |
|---|---|---|---|---|---|
| FeSn | Deville & Caron | 1858 | (47) | Yes | |
| | Headden | 1892 | (48) | Yes | From smelting processes. |
| | Edwards & Preece | 1931 | (49) | Yes | Thermal diagram. |
| | Ehret & Westgren | 1933 | (50) | Yes | Thermal X-ray diagram, provisionally identified as $\beta$. |
| | Ehret & Gurinsky | 1943 | (51) | Yes | Thermal X-ray diagram. |
| $FeSn_2$ | Nöllner | 1860 | (52) | Yes | Residue from dissolving tin in acid. |
| | Headden | 1892 | (48) | Yes | From smelting processes. |
| | Edwards & Preece | 1931 | (49) | Yes | Thermal diagram. |
| | Ehret & Westgren | 1933 | (50) | Yes | Thermal X-ray diagram. |
| | Pingault | 1934 | (53) | Yes | Prepared from Sn & $FeCl_2$. |
| | Ehret & Gurinsky | 1943 | (51) | Yes | Thermal X-ray diagram. |
| | Wollbaum | 1943 | (54) | Yes | X-ray data. |
| | Nowotny & Schubert | 1943 | (55) | Yes | X-ray data. |
| $\alpha$-$FeSn_2$ | Wever & Reinecken | 1926 | (56) | Yes | Thermal diagram. |
| $\beta$-$FeSn_2$ | Wever & Reinecken | 1926 | (56) | No | Thermal diagram. |
| $\gamma$-$FeSn_2$ | Wever & Reinecken | 1926 | (56) | No | Thermal diagram. |
| $\delta$-$FeSn_2$ | Wever & Reinecken | 1926 | (56) | No | Thermal diagram. |
| $FeSn_3$ | Spencer | 1921 | (57) | No | |
| $FeSn_5$ or $FeSn_6$ | Rammelsberg | 1863 | (58) | No | |
| $Fe_2Sn$ | Edwards & Preece | 1931 | (49) | Yes | Thermal diagram. |
| | Russell, Kennedy et al. | 1932 | (59) | Yes | Electrolyze Fe into Sn amalgam. |
| | Ehret & Westgren | 1933 | (50) | Yes | Thermal X-ray diagram, provisionally identified as $\beta''$. |
| | Ehret & Gurinsky | 1943 | (51) | Yes | Thermal X-ray diagram. |
| $Fe_2Sn_2$ | Headden | 1892 | (48) | No | From smelting processes. |
| $Fe_3Sn$ | Lassaigne | 1930 | (46) | No | Isolated from Fe distilling retort. |
| | Headden | 1892 | (48) | No | From smelting processes. |
| | Wever & Reinecken | 1926 | (56) | No | Thermal diagram |
| | Nial | 1943 | (60) | No | X-ray data. |
| $Fe_3Sn_2$ | Ehret & Gurinsky | 1943 | (51) | Yes | Thermal X-ray diagram. |
| $Fe_3Sn_4$ | Berthier | 1863 | (61) | No | |
| | Headden | 1892 | (48) | No | From smelting processes. |
| $Fe_4Sn$ | Bergmann | 1897 | (62) | No | Prepared from an alloy. |
| | Berthier | 1863 | (61) | No | |
| | Headden | 1892 | (48) | No | From smelting processes. |
| $Fe_5Sn$ | Russell, Kennedy et al. | 1932 | (59) | No | Electrolyze Fe into Sn amalgam. |
| $Fe_5Sn_6$ | Headden | 1892 | (48) | No | From smelting processes. |

| Formula | Author | Date | No. | Gurinsky | Remarks |
|---|---|---|---|---|---|
| FeSn | Deville & Caron | 1858 | (47) | Yes | |
| | Headden | 1892 | (48) | Yes | From smelting processes. |
| | Edwards & Preece | 1931 | (49) | Yes | Thermal diagram. |
| | Ehret & Westgren | 1933 | (50) | Yes | Thermal X-ray diagram, provisionally identified as $\beta$. |
| | Ehret & Gurinsky | 1943 | (51) | Yes | Thermal X-ray diagram. |
| $FeSn_2$ | Nöllner | 1860 | (52) | Yes | Residue from dissolving tin in acid. |
| | Headden | 1892 | (48) | Yes | From smelting processes. |
| | Edwards & Preece | 1931 | (49) | Yes | Thermal diagram. |
| | Ehret & Westgren | 1933 | (50) | Yes | Thermal X-ray diagram. |
| | Pingault | 1934 | (53) | Yes | Prepared from Sn & $FeCl_2$. |
| | Ehret & Gurinsky | 1943 | (51) | Yes | Thermal X-ray diagram. |
| | Wollbaum | 1943 | (54) | Yes | X-ray data. |
| | Nowotny & Schubert | 1943 | (55) | Yes | X-ray data. |
| $\alpha$-$FeSn_2$ | Wever & Reinecken | 1926 | (56) | Yes | Thermal diagram. |
| $\beta$-$FeSn_2$ | Wever & Reinecken | 1926 | (56) | No | Thermal diagram. |
| $\gamma$-$FeSn_2$ | Wever & Reinecken | 1926 | (56) | No | Thermal diagram. |
| $\delta$-$FeSn_2$ | Wever & Reinecken | 1926 | (56) | No | Thermal diagram. |
| $FeSn_3$ | Spencer | 1921 | (57) | No | |
| $FeSn_5$ or $FeSn_6$ | Rammelsberg | 1863 | (58) | No | |
| $Fe_2Sn$ | Edwards & Preece | 1931 | (49) | Yes | Thermal diagram. |
| | Russell, Kennedy et al. | 1932 | (59) | Yes | Electrolyze Fe into Sn amalgam. |
| | Ehret & Westgren | 1933 | (50) | Yes | Thermal X-ray diagram, provisionally identified as $\beta''$. |
| | Ehret & Gurinsky | 1943 | (51) | Yes | Thermal X-ray diagram. |
| $Fe_2Sn_2$ | Headden | 1892 | (48) | No | From smelting processes. |
| $Fe_3Sn$ | Lassaigne | 1930 | (46) | No | Isolated from Fe distilling retort. |
| | Headden | 1892 | (48) | No | From smelting processes. |
| | Wever & Reinecken | 1926 | (56) | No | Thermal diagram |
| | Nial | 1943 | (60) | No | X-ray data. |
| $Fe_3Sn_2$ | Ehret & Gurinsky | 1943 | (51) | Yes | Thermal X-ray diagram. |
| $Fe_3Sn_4$ | Berthier | 1863 | (61) | No | |
| | Headden | 1892 | (48) | No | From smelting processes. |
| $Fe_4Sn$ | Bergmann | 1897 | (62) | No | Prepared from an alloy. |
| | Berthier | 1863 | (61) | No | |
| | Headden | 1892 | (48) | No | From smelting processes. |
| $Fe_5Sn$ | Russell, Kennedy et al. | 1932 | (59) | No | Electrolyze Fe into Sn amalgam. |
| $Fe_5Sn_6$ | Headden | 1892 | (48) | No | From smelting processes. |
| $Fe_9Sn$ | Headden | 1892 | (48) | No | From smelting processes. |
| $\beta'$ | Ehret & Westgren | 1933 | (50) | No | Thermal X-ray diagram, uncertain composition. |
| $\gamma$ | Ehret & Westgren | 1933 | (50) | Yes | Thermal X-ray diagram, solid solution. |
| | Ehret & Gurinsky | 1943 | (51) | Yes | Thermal X-ray diagram, solid solution. |

III. The System Iron-Tin:

The first constitutional diagram for the Fe-Sn system was that published by Isaac & Tammann[1] in 1907 (Fig.4). This work can not be considered as any more than an initial review of the system. These workers used thermal analysis in conjunction with microscopic study and magnetometric tests.

The essential salient points of their diagram are:

1. Miscibility gap, based on 1140°C. and stretching from 50 to 89% Sn.
2. Steep liquidus curve from 89% Sn to 100%. The only solubility figures given are 7.5% Fe at 1050°, 5% at 968°, and 2.5% at 833°C.
3. Solid solution as the stable solid phase between 893° and 1140°C.
4. A compound of unknown composition stable from 780° to 893°C. Isaac & Tammann suggested that it might correspond to $Fe_3Sn$.
5. A polymorphic change from the $\beta$ to the $\gamma$ form of the above compound at 780°C.
6. Either the $\alpha$-form of this compound or a new compound stable below 496°C.

Wever & Reinecken[56] disputed the existence of a miscibility gap in the system. Although they could not

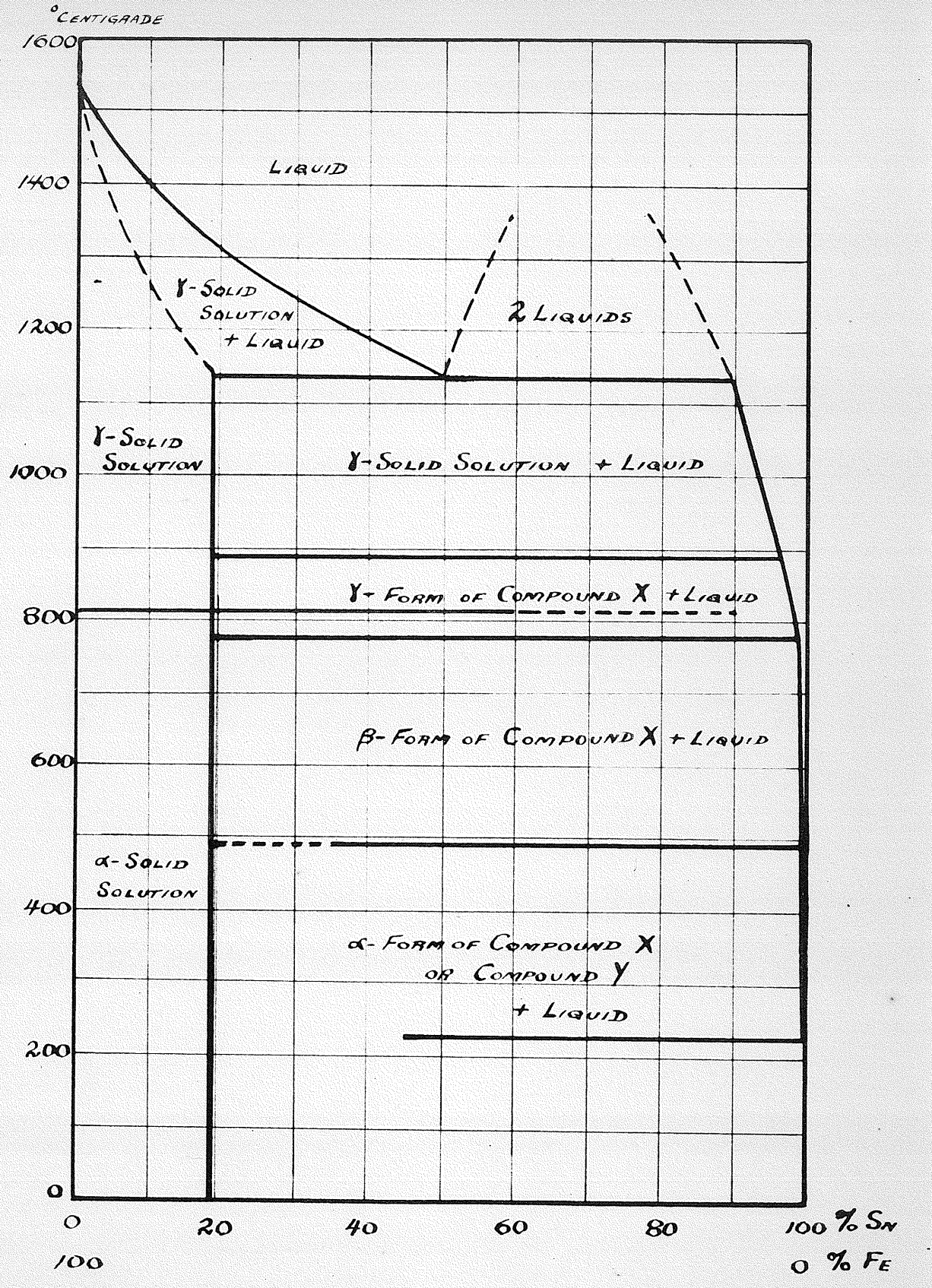


FIG. 4 ISAAC & TAMMANN (1907)

prevent the formation of two layers, they refused to recognize this as a stable condition and attributed it to liquation. The apparent basis of their conclusion is the failure of thermal analysis to detect an arrest above 1140°C. in the region of 50-89% Sn. Citing Ruer & Goerens'[64] paper on Iron-Copper, in which the authors stated that the miscibility gap in that system will not appear for pure materials, Wever & Reinecken claimed that, by analogy, there should be no gap in the system Fe-Sn, and that liquation was the cause of the two apparent layers.

As stable intermetallic compounds, they recognized only $Fe_3Sn$ which decomposes at 890°C. and four polymorphic forms of $FeSn_2$ in their diagram (Fig.5).

On purely theoretical grounds Wever & Reinecken introduced a line slightly below 890°, indicating that $Fe_3Sn$ and $\delta$-$FeSn_2$ together form a stable phase region from 42-82% Sn. They gave no experimental evidence to support this double transition line at 890°.

Also, Wever & Reinecken investigated the effect of tin on the $\alpha$-$\gamma$ transformation of iron; in this transition they observed a considerable difference between heating and cooling curves. A more detailed study of the $\alpha$-$\gamma$ transition was later published by Wever[65].

Wever & Reinecken set the maximum solid solubility of Sn in Fe at 18-19%. However, they added no new

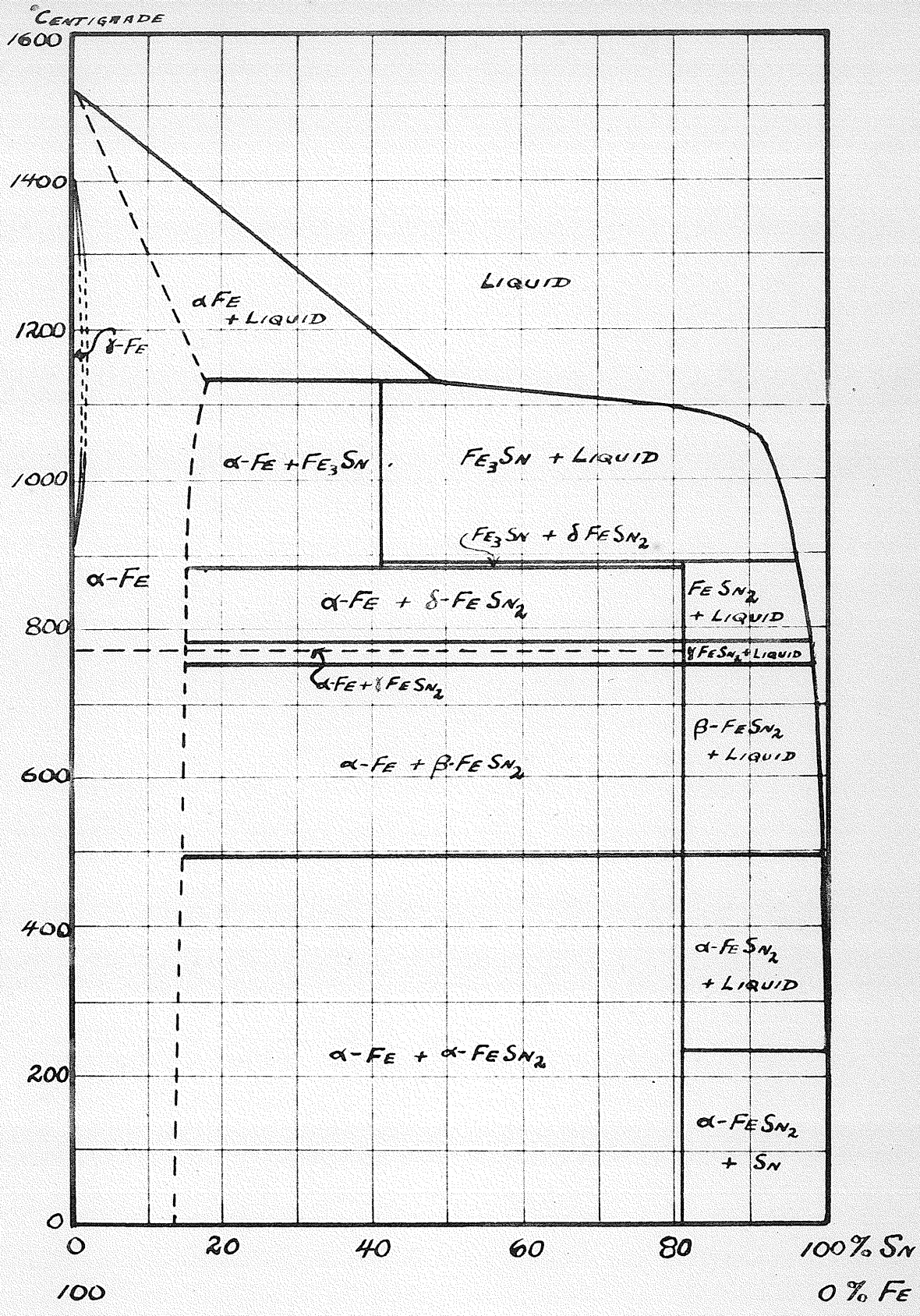


FIG. 5 WEVER & REINECKEN (1926)

information of significance on the lay of the liquidus curve from 89% to 100% Tin, since the only values they gave in their data were very badly scattered.

In view of the origin of this research problem, it is interesting to note that Wever & Reinecken said: "The refining of high-tin containing alloys results satisfactorily through filtration at just over 240°C."

Ruer & Kuschman[66] immediately challenged the allegation by Wever & Reinecken that the miscibility gap is non-existent in both the Fe-Sn and the Fe-Cu systems. These authors denied the interpretation placed on the work of Ruer & Goerens and implied that carbon, as an impurity, merely facilitated the ready formation of two layers, but did not create them.

They claimed, beyond any question, the formation of two layers for both the Fe-Sn and Fe-Cu systems, when using very pure materials. The basis of their claim was the presence, in a melt cooled from a temperature far above the base of the alleged miscibility gap, of two distinct layers of different compositions. However, in the case of Fe-Cu, the lack of a miscibility gap for pure materials has also been suggested by other workers.[67] It has been claimed that a 50-50 mixture of Fe and Cu forms a homogeneous liquid at temperatures just above the liquidus curve, but that upon further heating, two immiscible liquids appear. Also, the addition of small amounts of foreign elements, such as carbon, causes the

removal of the region of homogeneity entirely.

Edwards & Preece[49] made the next thorough investigation of the equilibrium diagram of this system, using thermal and microscopic methods. They, too, claimed the existence of a miscibility gap for the system (Fig.6). However, it should be pointed out that as a result of the experimental procedure outlined in their paper, all of the alloys studied would have had a high percentage of carbon. As already mentioned, the presence of carbon is claimed to lead to the formation of a miscibility gap in the system Fe-Cu. Accordingly, their evidence, likewise, cannot be considered as conclusive proof of the presence of a miscibility gap on the liquidus curve for the pure components.

Their diagram did not recognize the existence of $Fe_3Sn$, and introduced $Fe_2Sn$ and FeSn, dispensing with the polymorphic transitions of $FeSn_2$, limiting the existence of the latter to temperatures below 496°C. In alloys of over 68% Fe, they did not recognize a transition at 750°C. as claimed by Wever & Reinecken.

With regard to the liquidus between 90% Sn and pure tin, no information is available since no experimental data whatever were given in the paper. Edwards & Preece, however, did state that in alloys containing as little as 0.01% Fe, the presence of needle-like crystals of $FeSn_2$ could be readily detected under the microscope. They claimed a maximum solid solubility of Sn in Fe to

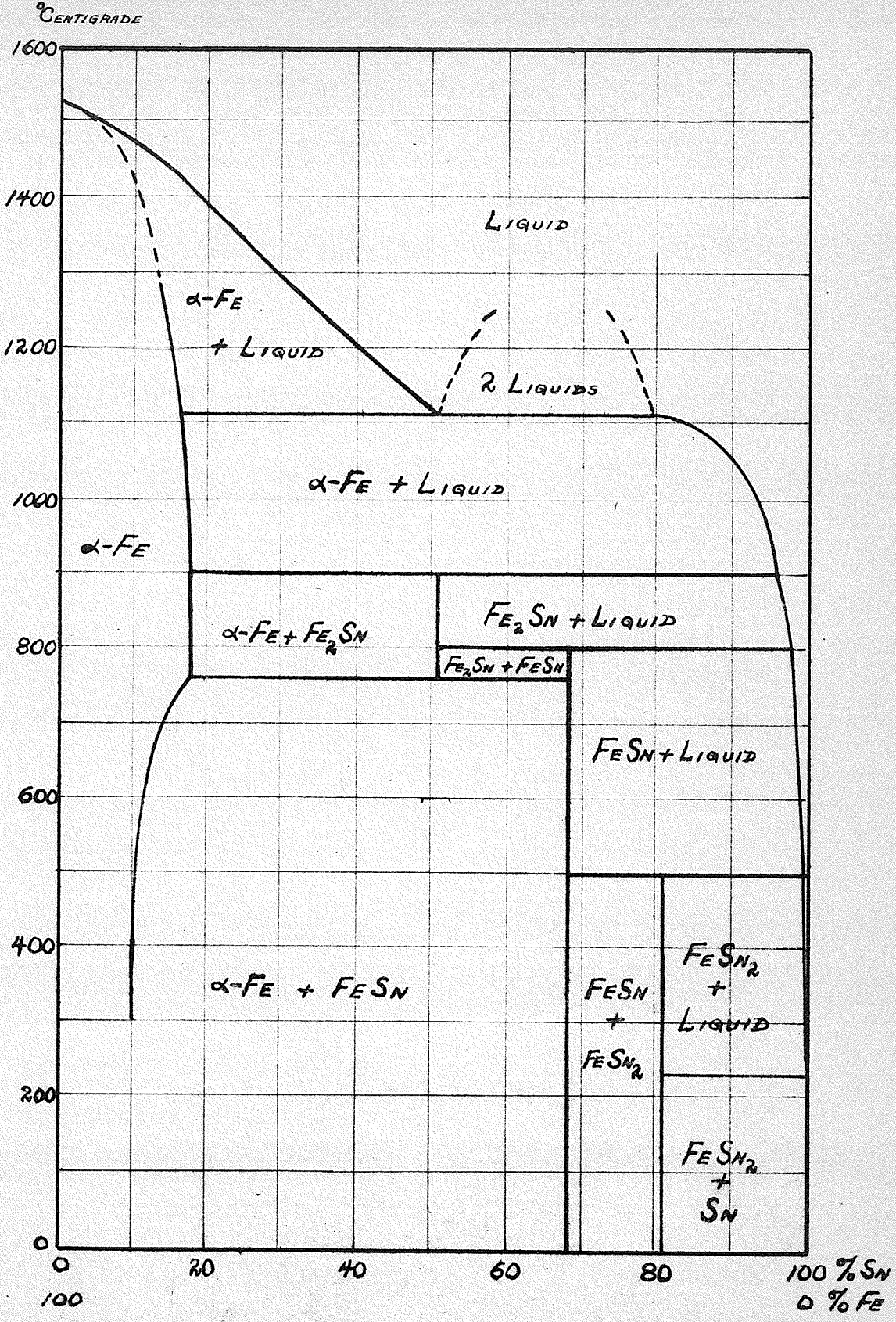


FIG. 6 EDWARDS & PREECE (1931)

occur at 760°C. (no value given).

Bannister[49], in discussing this work, also supported Edwards & Preece's claim for the existence of a miscibility gap, without, however, giving his reasons for this conclusion.

Bannister & Jones[68], studying the diffusion of tin into iron, stated the solid solution contains 15.2% Sn at 700°, and 18% at 1132°C.

In 1931, Westgren[34] gave some preliminary figures on work being done by Ehret. He reported, on the basis of X-ray studies, that a sample from the region $Fe_3Sn$ in the diagram of Wever & Reinecken contained $\alpha$-Fe and a phase with a NiAs type structure. He also provisionally reported the existence of other new solid phases, without giving details. A minimum value for the solid solubility of Sn in Fe was set at 12.1% at 900°C.

In 1933 Ehret & Westgren[50] gave more detailed results of their powder diffraction X-ray investigation. Their diagram is shown in Fig.7. They found the solid solubility of Sn in Fe to be 9.8% at 680° and 18.8% at 900°C.

Besides the phases reported by Edwards & Preece, Ehret & Westgren claimed $\beta'$ and $\gamma$ phases. The phases found by the latter, as shown in Fig.7, are:

$\alpha$ - $\alpha$-iron with tin present in solid solution.

$\beta$ - corresponds to FeSn of Edwards & Preece.

$FeSn_2$ - same phase region as for Edwards & Preece.

$\beta'$ - undeterminable - possibly two phases, but doubted,

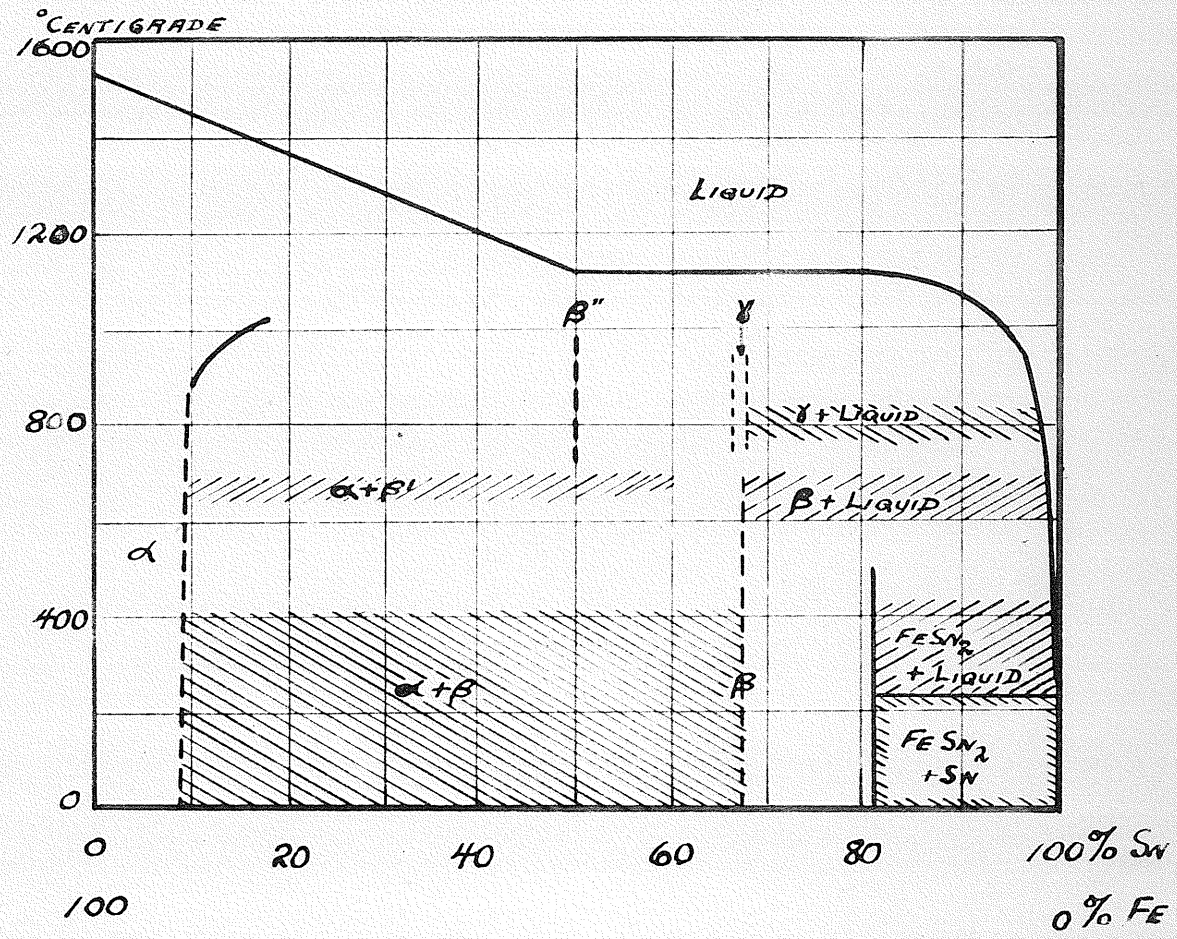


FIG. 7 EHRET & WESTGREN (1933)

$\beta''$- corresponds to $Fe_2Sn$ of Edwards & Preece.

$\gamma$- A nickel arsenide type structure of uncertain and possibly variable composition.

Jones & Hoare[2], using primarily microscopic methods, confirmed the existence of $Fe_2Sn$, FeSn, and $FeSn_2$, but they could not find evidence for the $\gamma$-phase of Ehret & Westgren.

Hanson, Sandford & Stevens,[27] in 1934, studied the effects of small amounts of Ag, Fe, Ni and As on tin. Although they conducted a thermal investigation of Ag-Sn, and Cu-Sn, and an isothermal of Ni-Sn, to determine the liquidus composition and the eutectic proportions, these workers did not attempt to investigate the liquidus of Fe-Sn. They did, however, report on the physical properties, e.g., tensile strength, of Sn containing small amounts of Fe.

A statement was made that at 1000°C., 5% of iron will dissolve in Sn. No experimental data were given to support this figure.

One statement made in this paper should be noted here, since the results of the present investigation could not confirm it. The authors, in replying to correspondence on their paper by W.A.Cowan[27] (who studied Cu-Sn), state that "iron.....has a very great effect on the melting point of tin."

Ehret & Gurinsky[51] in 1943 published the results of a very intensive X-ray powder diffraction investigation.

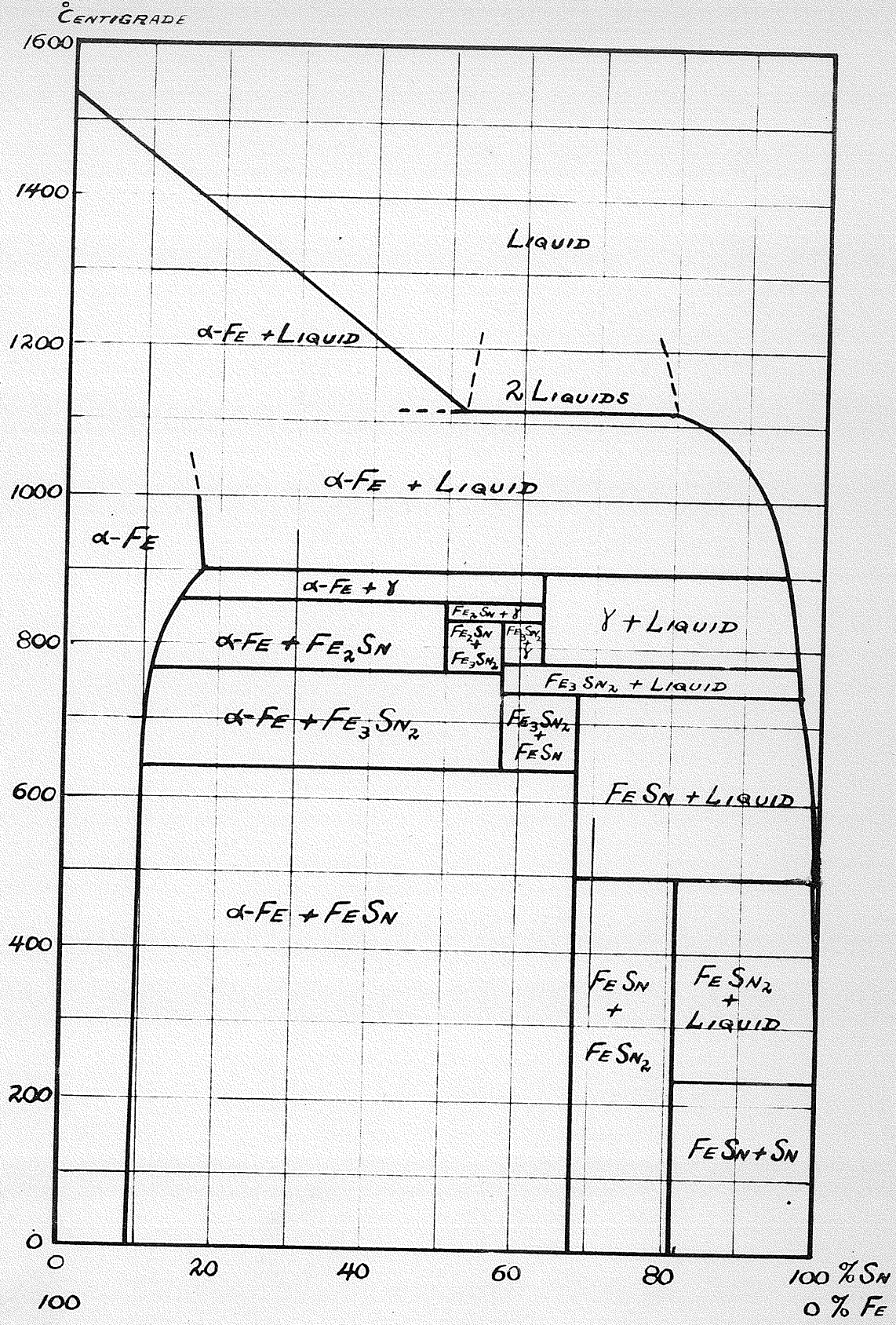


FIG. 8 EHRET & GURINSKY (1942)

Their diagram (Fig.8) had only one indeterminable phase, and at the same time introduced $Fe_3Sn_2$ as a new stable phase (the $\beta'$ of Ehret & Westgren). The $\gamma$-phase was reported as a complicated solid solution of the type common to systems involving a combination between transitional elements and elements with large atoms. It has a NiAs type structure.

Unfortunately, Ehret & Gurinsky made no serious attempt to fix the horizontal borders for their phases, and thus the temperatures used in the diagram must be, for the present, those of the previous thermal investigations.

Undoubtedly, the most reliable phase diagram of the Fe-Sn system is the X-ray diagram of Ehret & Gurinsky[51] using the temperature boundaries suggested by the earlier thermal investigations, specially those of Wever & Reinecken[56]. For the boundaries of the $\gamma$-Fe region, the only work published is that of Wever[65].

For iron containing some graphite, the presence of the miscibility gap would appear to be beyond question. For mixtures of pure iron and tin, however, the claim of Wever & Reinecken (although not their explanation) cannot be dismissed in view of the acceptance of the Fe-Cu diagram[67] in which, for pure Fe and Cu, the immiscibility of the two liquids does not begin until the temperature is somewhat above that of the liquidus.

# EXPERIMENTAL

# EXPERIMENTAL

## I. Introduction:

The study of this system may be divided into several sections:

(1) The liquidus from 1140° (89% Sn) to 232°C. This portion of the liquidus is very steep, and forms the principal subject of this investigation.

(2) The composition of the eutectic at 232°. This had not been previously investigated.

(3) The miscibility gap. The existence of the gap on the liquidus, in contrast to a region of immiscibility above the liquidus, should be confirmed for pure materials, and its boundaries determined. Time did not allow this work to be undertaken. G.B.Skinner[69] is constructing a tungsten-wound furnace[70] to investigate this region. Since such a furnace operates in an atmosphere of cracked ammonia[71], there will be no contamination of the metals.

(4) The liquidus from 100% Fe to 50% Fe. This region has been quite accurately mapped, and need not be repeated.

(5) The solid phases present. These have been adequately investigated by previous workers, especially Ehret & Gurinsky[51].

II. Purity of Materials Used:

For the study of the eutectic composition of tin, spectroscopic tin, obtained from the Vulcan Detinning Works of Sewaren, N.J., was used. No batch analysis was available, although it was stated by the manufacturers that Lucius Pitkin Inc. had analyzed previous batches prepared by the same method, and reported:

| | | | |
|---|---|---|---|
| Pb | .0005% | Au | .0005% |
| Fe | .0015% | As | .0001% |
| Sb | <.0001% | Bi | <.0001% |
| Ag | <.0001% | In | None found. |
| Pb, Cu, & Fe combined | .00025% | As & Sb combined | .0001% |
| Bi, Ag, & In combined | .0001% | | |

Sn (by difference) 99.9973%

For the study of the liquidus, Batch #73 of Vulcan "Commercial" tin was used. The following analysis was supplied with this:

| | |
|---|---|
| Fe | .0020% |
| Pb | Trace |
| Sb | .0023% |
| Cu | Trace |

Sn (by difference) 99.9957%

For the eutectic, Kahlbaum Reduced Iron was used. This was found to be the best of the reduced iron available. It was analyzed for total iron by titration with $K_2Cr_2O_7$, and was found to contain 95.4% Fe. Assuming the difference to be oxygen present as $Fe_3O_4$, this corresponds to 89.3% free iron. The Kaulbaum iron was analyzed for free iron, using the method of Christensen[72] (see Methods of Analysis), and gave 90.4% metallic Fe.

For the study of the liquidus, "Iron Wire for Standardization" was used. The Merck wire (fine wire on spools) was stated to contain at least 99.8% Fe, and the Cenco wire (thin 3" rods) was 99.7% Fe.

III. Methods of Chemical Analysis:

The free metallic iron content of the reduced iron was determined by the method of Christensen[72]. Half a gram of weighed sample was placed in a 100 cc. graduated flask filled with $CO_2$. 5 grams of $FeCl_3$, dissolved in 50 cc. freshly boiled water, were added. The flask was then warmed to about 50°C. and shaken for 15-20 minutes. The sample was then diluted to volume with freshly boiled water and kept under $CO_2$ overnight. 20 cc. portions were then titrated with .1N $KMnO_4$ in the presence of 20 cc. of 7N $H_2SO_4$, and 10 cc. of Rheinhart-Zimmerman Solution. The equation for the reaction is:

$$Fe + 2FeCl_3 \longrightarrow 3FeCl_2$$

Iron, in tin samples, was determined colormetrically using the blood-red color developed by KCNS with ferric iron. The following procedure was developed as suitable for all samples analyzed, since the tin never under-went hydrolysis on standing, and since sulphur never formed in the colormetric determination.

5 grams of tin were dissolved in 30 cc. concentrated HCl. Mellor[73] states that at least twice as much acid as $SnCl_2$ must be present to obtain an appreciable reaction rate. The solution may be heated to hasten the dissolving of the tin. The sample was then diluted with water to volume in a 200 cc. standard flask. Normally, 20 cc. of

this solution were placed in a 100 cc. Erlenmeyer, along with 10 cc. of 1:1 HCl and 10 cc. of 3% $H_2O_2$. A small filter funnel was put, stem downwards, in the neck of the flask, and the solution heated to just below boiling until the gas evolution had ceased.

The sample was cooled, washed into a 100 cc. standard flask with 40 cc. of 1:1 HCl and diluted to volume.

Comparison standards were made of pure tin. This was made from 25 grams of pure tin dissolved in 150 cc. concentrated HCl and diluted to 1 litre, thus giving the same concentration of Sn as present in the 200 cc. flasks. For every set of analyses, standards were prepared simultaneously, using the above standard stock solution. To the 20 cc. samples of pure tin, the required amounts of highly diluted standard Fe solutions were added to give a comparison standard of approximately the same composition as the unknown.

A 25 cc. portion of the oxidized sample and of the comparison standard were pipetted into dry 100 cc. beakers, each containing 10 cc. of 1:1 HCl. 5 cc. of 4N KCNS were then added to each, the solution stirred, and immediately examined under the colorimeter. A Bausch & Lomb Colorimeter of the Duboscq Type was used. Since the pure tin contained .002% Fe, a correction for this was required in some analyses where the iron content of the sample was very low.

For very dilute solutions, 40 cc. of the $SnCl_2$ solution were analyzed, and for stronger solutions only 10 cc.

The large excess of chloride ion prevented any interference due to variations in concentration. Moreover, the high acid concentration prevented hydrolysis of tin in samples kept for some time. It is necessary to boil off excess $H_2O_2$ before addition of KCNS, as otherwise the formation of colloidal sulphur prevents accurate determinations, also the odour of $H_2S$ and HCN may be observed from such solutions.

For work over 1% Fe, a volumetric method was developed which could be run on the unused portion of the $SnCl_2$ solution. The desired aliquot was oxidized with $Cl_2$ from a chlorine generator until the solution started to change to the green color of ferric iron. Chlorine was used as it was found the easiest oxidizing agent to remove quickly without resorting to excessively long boiling. The oxidized solution was then warmed and 15% stannous chloride solution added drop by drop, with constant stirring until the last shade of green disappeared. This procedure also served to remove any excess chlorine present. Bromine was not found suitable to use as its oxidation potential is too low to allow titration with any form of the diphenylamine indicator, the diphenylamine indicators being the only internal indicators having a suitable oxidation potential.

The standard method of iron analysis was then followed. The solution was cooled and 10 cc. of 3% $HgCl_2$ were added rapidly to remove excess stannous ion. The solution was then diluted, washed into a litre beaker, 10 cc. of syrupy $H_3PO_4$ and 15 cc. concentrated $H_2SO_4$ added, and the whole diluted to 700 cc. 6 drops of .2% solution of barium diphenylamine sulphonate were added. The solution was titrated with .01N $K_2Cr_2O_7$ to the violet color change. Using this concentration of $K_2Cr_2O_7$, Kolthoff & Sandell[74] state that a correction of .24 cc. must be subtracted from the titration as an indicator blank. Check results were obtained using pure Sn to which known amounts of Fe had been added.

The phosphoric acid is added to reduce the oxidation potential of the iron. The dilution is necessary to reduce the chloride ion concentration to less than 2N. Above that concentration, chloride ion is oxidized by $K_2Cr_2O_7$.

Usually the solution begins to hydrolyze as the titration is completed. This could probably be prevented by the addition of even more sulphuric acid, but the hydrolysis does not interfere with the end point of the titration.

There appears to be no reason why the above method, perhaps modified somewhat, will not be suitable for any concentrations in the Fe-Sn system.

A brief investigation was made to determine whether tin could be readily dissolved in $H_2SO_4$ in order to eliminate the necessity of dilution. According to Mellor[75], with $H_2SO_4$, sulphur is formed readily in the reaction with tin if the acid is too concentrated. In practice it was found that the rate of solution was too slow to be suitable for analysis. Accordingly, the best method of analysis of iron appears to be a volumetric determination of a highly diluted sample previously dissolved in HCl.

IV. Temperature Measuring Instruments:

In the eutectic investigation, mercury thermometers were used; one, a 0 - 360°C. thermometer, gave the temperature of the melt, and the other, a Beckmann, the changes in the temperature of freezing of Sn.

In all other work, a platinum - platinum 10%rhodium thermocouple was used. This thermocouple was calibrated frequently, during use, against the following points:

| | | |
|---|---|---|
| Sn | Freezing Point | 231.9°C. |
| Pb | " " | 327.4 |
| Zn | " " | 419.4 |
| Al (99.95%) | " " | 659.9 |
| NaCl | Melting Point | 800.4 |
| Ag | Freezing Point | 960.5 |

The variation of the e.m.f. of a Pt - Pt 10%Rh thermocouple with temperatures were plotted on a very expanded scale using the data given in "Temperature - Its Measurement and Control in Science and Industry"(76). The calibration point e.m.f.'s obtained were plotted on the same graph, thus allowing the shape of the standard curve to be used as a guide in the drawing of the calibration curve.

The thermocouple was used in conjunction with a Leeds & Northrup Type K-1 Potentiometer and a Leeds & Northrup Type P Wall Galvanometer of sensitivity .0015 $\mu$ amps./mm. This gave an uncertainty in e.m.f. readings of less than

5 microvolts (corresponding to about 1/2°C.). Thus all temperatures could be measured to within ± 1°C.

It will be seen from Fig. 10 and Fig.15 that instead of using a cold junction of Pt - PtRh, two cold junctions, a Cu-Pt and a Cu-PtRh, were used. This made no difference in the voltage of the thermocouple (Law of Successive Contacts), but did provide more convenient connections for the wiring of the circuit.

During the work on thermal analysis (pages 44-48) the cold junction was a water bath at room temperature. However, over a twenty-four hour period the room temperature fluctuated over a 10°C. range. Accordingly, for the isothermal analysis (pages 49-66) it was necessary to thermostat the water bath. A temperature of 32°C. was used, as this was above any possible fluctuation in room temperature.

## V. Determination of Eutectic Composition:

### A. Apparatus:

For the investigation of the eutectic composition of $FeSn_2$ in Sn, the apparatus shown in Fig. 9 was used. The two thermometers were jacketed with Pyrex cases in order to protect the thin-walled thermometers from the strains encountered during the solidification of the molten tin. Mercury was used in the casing to provide efficient heat transfer between it and the thermometer. The Beckmann thermometer used had a range of 5-1/2°C; the ordinary thermometer had a range of 0°-360°C.

It should be noted that all glass in contact with the melt was of Pyrex, to minimize the leaching action of molten tin on the glass.

The 6x2" Pyrex tube was suspended inside a piece of tile pipe (4-1/2" internal diameter), on the outside of which was wound a nichrome heating element. This element was insulated on the outside with a 1/2" layer of asbestos powder, and with asbestos paper. The furnace was placed at the centre of two concentric sheet metal cylinders closed at the bottom. These were of 6" and 10-3/4" diameter. Cold tap water was circulated in the annulus between the two cans. Over the whole was a tight fitting lid, a piece of Transite asbestos board with a 2" diameter hole through which the tube was suspended in the furnace. This Transite board is heat resistant and electrically non-conducting. The power leads to the furnace were connected to this board.

A stream of pure nitrogen was circulated over the melt at all times. The gas, obtained from commercial cylinders (99.8% $N_2$), was purified by

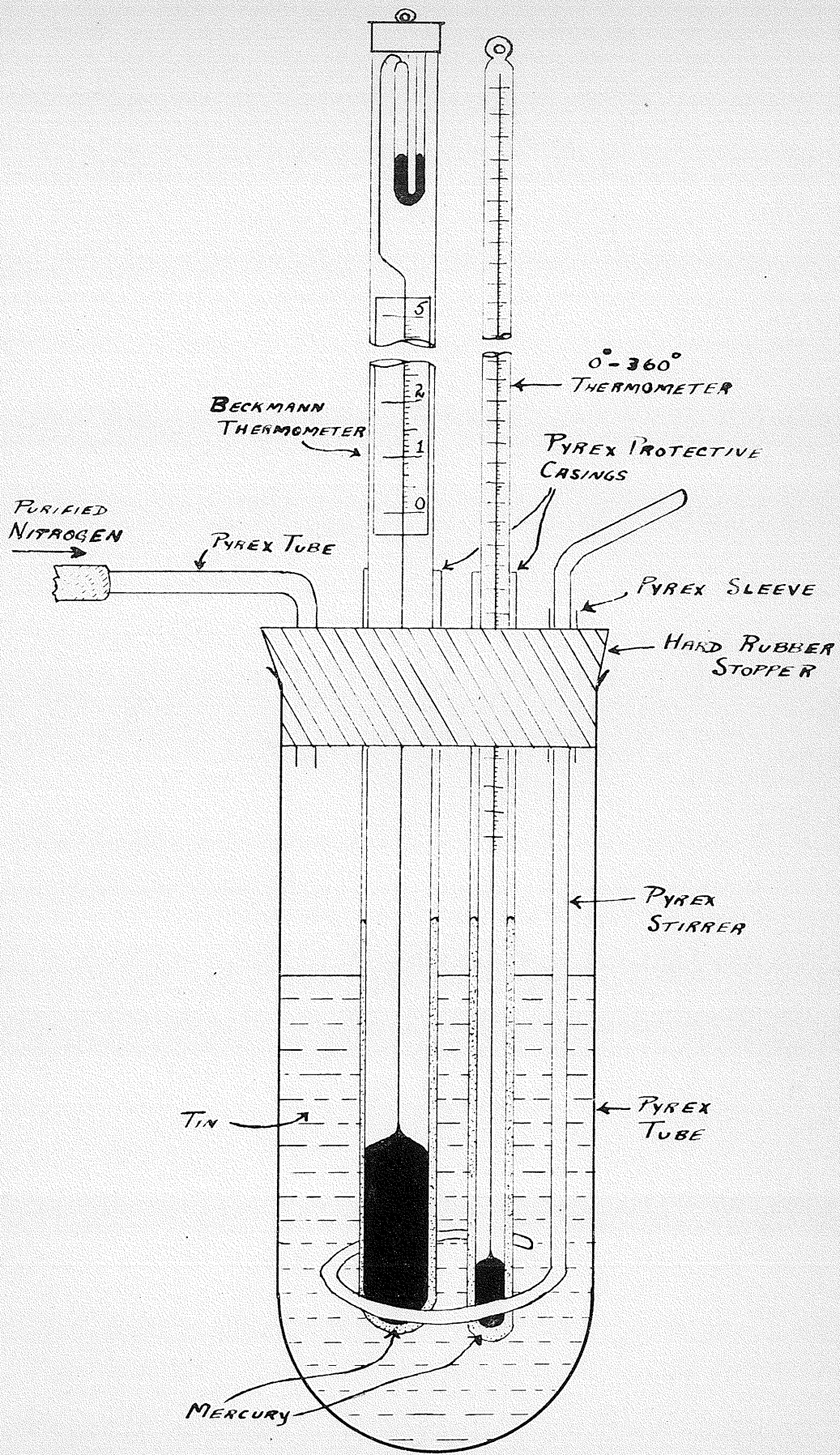
0°-360°
THERMOMETER
BECKMANN
THERMOMETER
PYREX PROTECTIVE
CASINGS
PURIFIED
NITROGEN
PYREX TUBE
PYREX SLEEVE
HARD RUBBER
STOPPER
PYREX
STIRRER
TIN
PYREX
TUBE
MERCURY

FIGURE 9

first passing it through pyrogallol solution, followed by a $CaCl_2$ drying tube. It was then passed through a long red-hot combustion tube containing freshly reduced copper wire and powder. The oxygen content of this purified nitrogen was not determined. It must, however, have been very low since practically no contamination of the molten tin was observed.

B. Procedure:

400 grams of spectroscopic tin were placed in the tube and then the system was thoroughly flushed with nitrogen to remove air. The sample was then heated to about 250°C. The Beckmann thermometer had been previously set so that the freezing point of tin occurred in the centre of the scale.

Repeated trials were made for the Beckmann thermometer readings during the solidification of the tin. Vigorous stirring was necessary to prevent excessive supercooling which, at times, amounted to as much as 12°C. A steady drift in Beckmann readings was observed over a period of one week. In order to minimize this drift, the thermometer was never touched during the run. Finally, however, a constancy of $\pm$ .005°C. was obtained in three trials over a period of 4 hours. 4 grams of Kahlbaum reduced iron were quickly added and the molten tin vigorously stirred, the temperature being kept at 250°C. for several hours. This was the highest temperature that could be used without destroying the setting on the Beckmann. Although constancy was obtained in the first trial after the addition of iron, the slow persistent drift in readings later appeared again.

It should be noted that Heycock & Neville[14] stated that even for a mercury thermometer which had been annealed for two weeks at 250°C., this creep still was present to the extent of .001°C. per day.

In view of the difficulty in working with a mercury thermometer under such conditions, further work along this line was abandoned.

During the calibration of the thermocouple for the work on thermal and isothermal analyses, several attempts were made to determine a possible difference in the freezing point of pure tin and that containing a large amount of dissolved iron. No such difference was ever obtained.

## VI. Thermal Analysis:

### A. Apparatus:

A small laboratory furnace 6-3/4 inches external, and 4-1/2 inches internal diameter, and 4 inches high, was used for this work. The single covered nichrome element of the furnace had a power consumption, on full load, of 900 watts. As may be seen from the schematic diagram of Fig.10, a bank of wire-wound low resistance rheostats were placed in series with the furnace. The circuit was so arranged that by throwing switch K-1 the resistance of the furnace and rheostat circuit could be quickly determined on a Wheatstone Bridge.

The furnace was placed at the centre of two concentric sheet metal cylinders closed at the bottom. These were of 10-3/4 inches and 17-3/4 inches diameter. Between the two cylinders, tap water was circulated. The furnace rested on 3/4 of an inch of asbestos, lining the bottom of the inner container. The furnace had its own close fitting lid. The Transite board, used in the previous experiment, was so cut that this lid would fit tightly into it.

Since the neutral body method of Roberts-Austen (see page 11) was used, two opposed thermocouples were required. As will be noted in Fig.10, the difference in voltage between the couples was read directly on galvanometer G-1 (a Leeds & Northrup Type 2400).

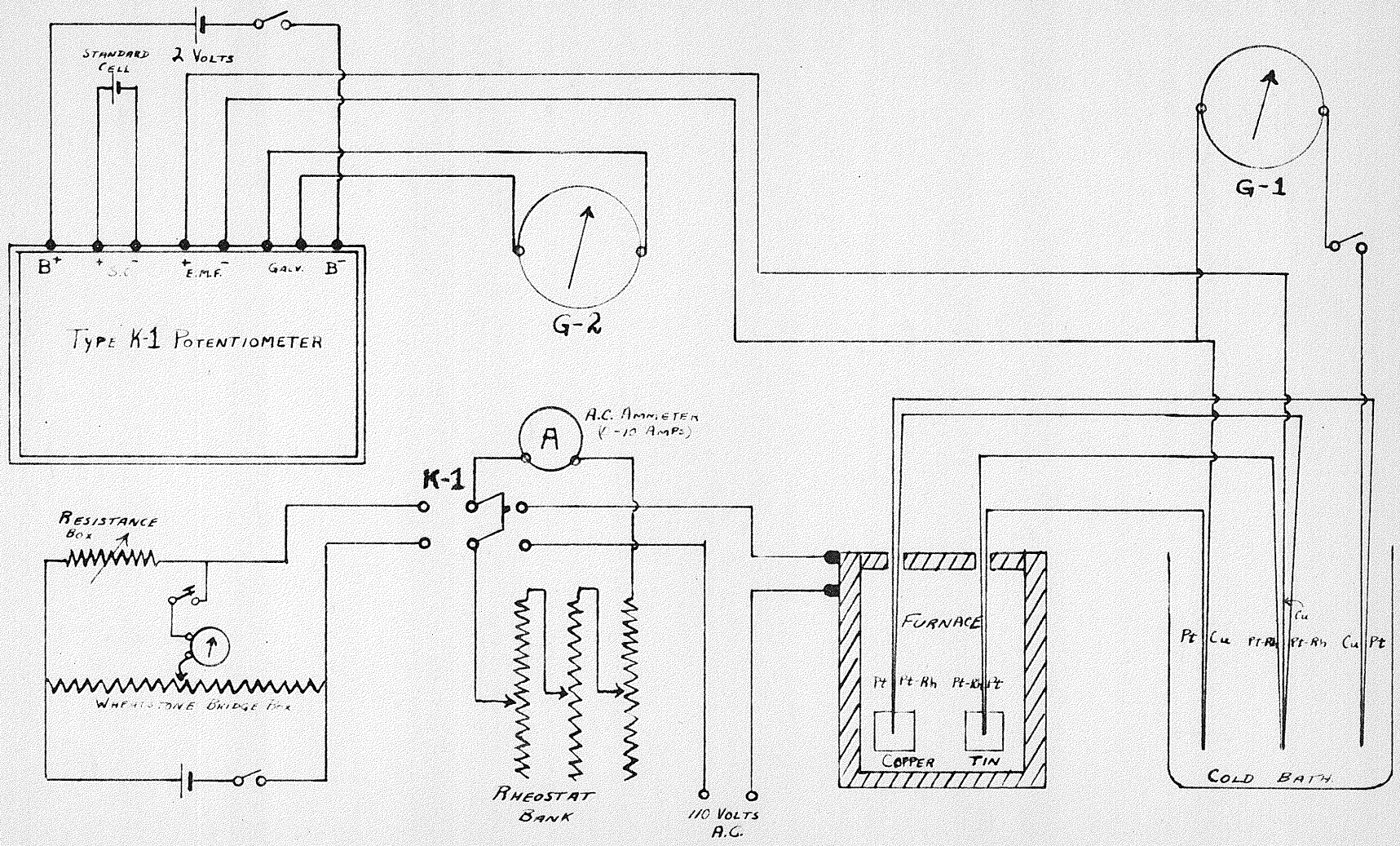
STANDARD CELL
2 VOLTS
B+
+ S.C. -
+ E.M.F. -
GALV.
B-
TYPE K-1 POTENTIOMETER
G-2
G-1
A.C. AMMETER (0-10 AMPS)
A
K-1
RESISTANCE BOX
WHEATSTONE BRIDGE BOX
RHEOSTAT BANK
110 VOLTS A.C.
FURNACE
Pt
Pt-Rh
Pt-Rh
COPPER
TIN
Pt Cu Pt-Rh Pt-Rh Cu Pt
Cu
COLD BATH

FIGURE 10

The constants of this galvanometer were given as:

Current sensitivity .003 $\mu$amps./mm. at 1 metre.

Resistance 529 ohms.

Calculated voltage sensitivity 1.62 $\mu$v./mm. at 1 metre.

The galvanometer was used with a reading telescope to which was attached a metre stick as a scale. As this telescope was used at a distance of 4-1/2 feet from the galvanometer, the above mentioned sensitivity was considerably enhanced.

As previously mentioned (page 39) the thermocouples were Pt - Pt 10%Rh, used in conjunction with a Type K-1 Leeds & Northrup Potentiometer and a Leeds & Northrup Type P Wall Galvanometer, G-2.

As 260 gram samples of Sn were used, the neutral body was a block of copper of weight 180 grams, this amount having the same heat content. The junction of the thermocouple was at the centre of this block.

Originally, the tin sample and the copper block were put in Vitreosil Silica Tubes, which were water cooled at the top so that they could be stoppered and the contents maintained under vacuum. However, crystallization of the silica occurred, and the method was, of necessity, abandoned. Instead, the sample was placed in a Salamander Graphite Crucible and covered with charcoal. The copper block was kept in a closed porcelain tube. The charcoal covering was used with the tin sample in an attempt to keep surface oxidation to a minimum.

B. Procedure:

For thermal analysis, conditions must be absolutely reproducible, trial by trial. For accuracy, it is not only necessary to have linear cooling of the furnace, but also absolute constancy of environment so that the Newtonian cooling effect is not a variable, changing with room temperature. This was achieved here by having tap water running continuously at a steady rate. The temperature of the running water is quite constant enough for the temperatures involved here.

It was first necessary to calibrate the furnace to give linear cooling. This was done by first determining the circuit resistance by the Wheatstone Bridge for various rheostat settings, the settings being measured distances from one end of the rheostat to the travelling tap. First, a run was made by heating the furnace to 1000°C. and then cutting off the heating current entirely. Temperature readings were taken every minute until the temperature had dropped to 225°C. The resultant plot of temperature against time allowed an initial estimate of the required heating currents to be made. A controlled cooling curve was then taken, adjustments being made every minute to the rheostat settings. All settings were made by measuring the position of the travelling tap from one end since the time margin was too small to allow

a potentiometer reading and a rheostat setting every minute unless the latter could be simplified to a quick motion. The plot of the values obtained in this run was used as a basis for the next trial. After several such trials, a very good straight line was obtained. The rate of cooling was determined by the slowest rate that the furnace would free-cool. Accordingly, a rate of about 3-1/3°C. a minute was used. This made the length of one run about 4-1/4 hours.

The thermal analysis of samples was then carried out. Initially, a blank on pure tin was run. Then the sample, in a Salamander Crucible as described above, had .056% Fe added to it in the form of fine Merck iron wire. The sample was held at 900°C. for about 10 hours. A cooling curve was then taken in the following manner. The furnace was linearly cooled by using the required adjustment every minute, potentiometer readings for the temperature of the sample also being made every minute. At the same time, another observer, seated at the reading telescope of galvanometer G-1 (Fig.10) recorded the corresponding reading. These scale readings are obviously a measure of the difference in temperature between the tin sample under investigation and the copper block.

Later, the iron content of the sample was increased to .5%, using Kahlbaum iron, and then to 3%.

The author wishes to acknowledge, here, his gratitude to the many students, both graduate and under-graduate,

who recorded the above galvanometer readings, as, without their assistance, the above procedure would have been physically impossible.

## VII. Isothermal Analysis:

### A. The Electronic Control Circuit:

#### 1. Introduction:

In order to carry out any isothermal investigation, some method of maintaining constant temperature must be provided. The thermo regulators in use for ordinary and moderate temperature ranges are not adaptable to furnace temperatures.

The thermal detector (i.e. the measuring and/or controlling element) is normally either a platinum resistance thermometer or a thermocouple. Since the former, and its accessories, were not available, a thermostat had to be prepared using a thermocouple as its detector.

The control used was designed for air-bath furnaces, electrically heated by wire-resistance elements, (A long time lag is an inherent characteristic when covered resistance elements are used.)

There are a number of temperature controls described in the literature[77,78,79] which will give a higher degree of precision, but which have limitations as to temperature range, variation in power imput to the furnace, or time lag.

The limitation in temperature range is usually imposed by the range of the platinum resistance thermometer. When a thermocouple is used as the temperature detector, the limit is determined by the refractory nature of the

elements employed. Thus, for a tungsten-molybdenum couple, temperatures in excess of 2000°C. may be controlled. The furnace being thermostatted in this investigation had a nichrome element, permitting operation up to 1000°C. However, a furnace employing tungsten windings is to be constructed by G.B.Skinner[69]. This will permit the attaining of any desired temperature up to 2000°C.

In previous circuits, a thyratron was used, in series with the furnace, as a current regulator by controlling the relative phase of the grid voltage. However, such circuits are not applicable over a wide range of power consumption, nor do they lend themselves readily to either frequent changes in the required temperature or to changes in the furnace windings. The regulation of temperature using the control to be described (Fig.11) has been simplified to two manual adjustments: the setting of the series resistance X for approximate temperature, and the adjustment of the opposing e.m.f. for the thermocouple (Resistance R).

Since this control uses a relay to shunt a portion (S) of the series resistance, it affords no practical limitation in the power delivered to the furnace. However, to gain in this respect, continuous control was sacrificed; the effect of discontinuous control may be minimized by keeping the shunted portion of the series resistance as small as possible.

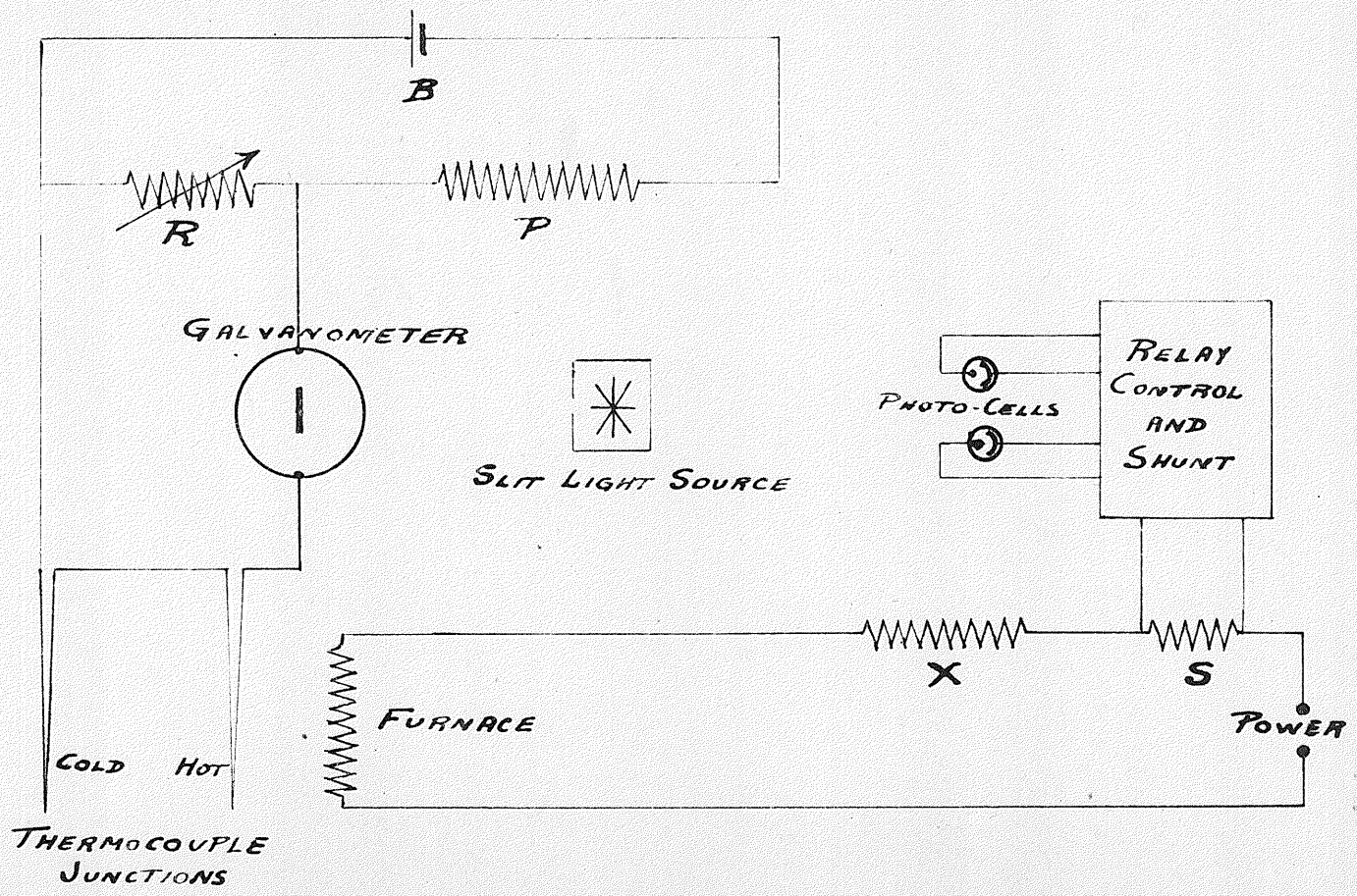
B
R
P
GALVANOMETER
SLIT LIGHT SOURCE
PHOTO-CELLS
RELAY CONTROL AND SHUNT
X
S
FURNACE
POWER
COLD
HOT
THERMOCOUPLE JUNCTIONS

FIGURE 11

The thyratron circuits depend upon the light intensity falling on a single photo-cell. It was felt that difficulties in maintaining a constant light source over long periods of time might arise. Also, with the single photo-cell there is the danger that an appreciable time lag in the furnace will cause the light to move completely off the cell, and thus all control would be lost. The chief advantage of this circuit is the use of two photo-cells, one being employed to open, and the other to close, the shunt. If the light beam passes either cell, the proper action is accomplished as it does so, and the light must eventually return to the opposite cell.

2. Description of the Circuit:

This control circuit was designed by Bruce C. Lutz, formerly of the Department of Physics.

In order to give a complete record for others who may later use the set constructed for this investigation, both a general summary and a rather more itemized description will be given.

(a) General Summary:

The circuit of Fig.12 consists of the following stages: the relay tube, a 6F6; an Eccles-Jordan circuit[80,81] consisting of two 6C5's; and two pulse circuits functioning alternately. Each of the latter consists

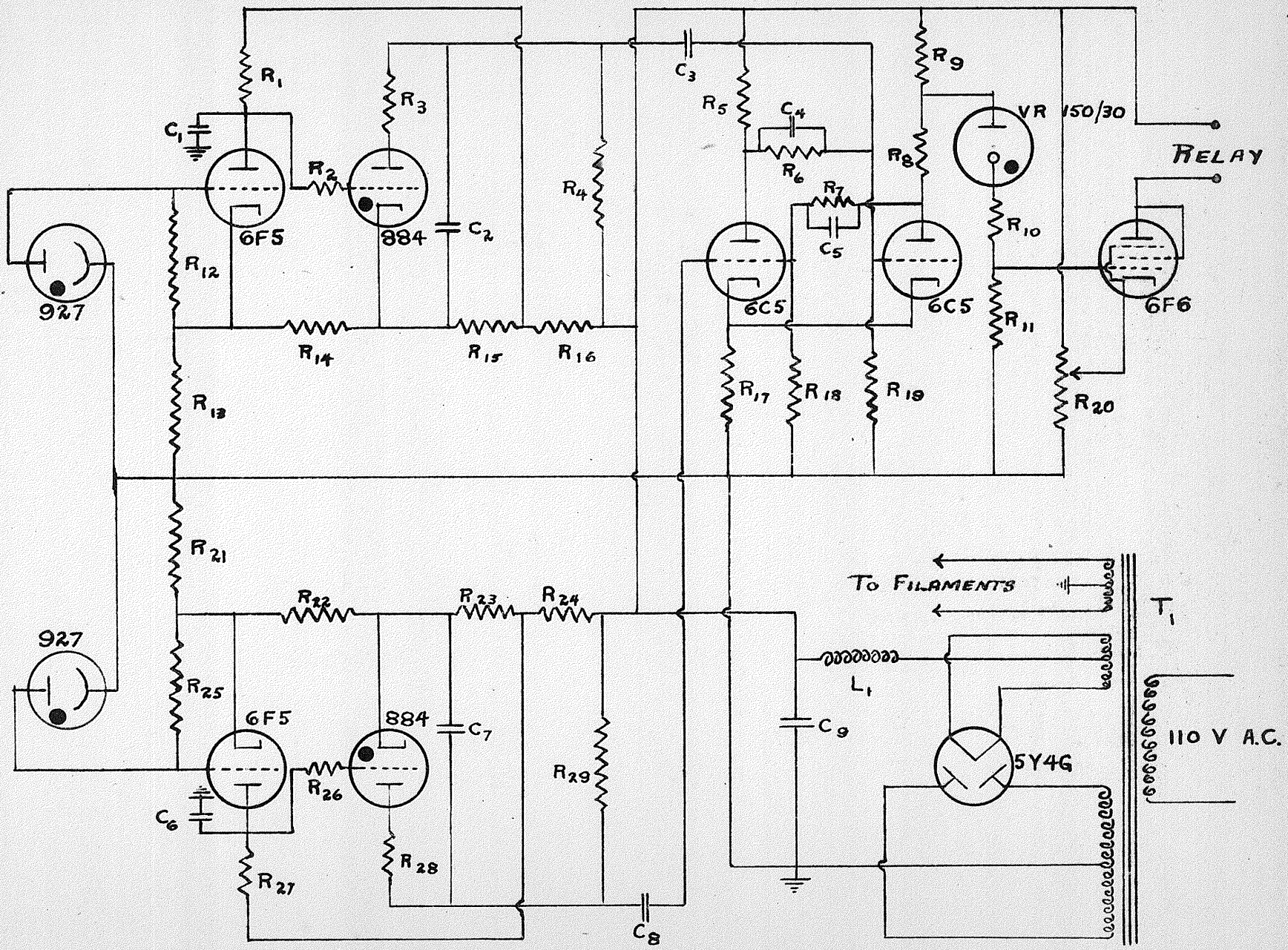
R1
C1
R3
R2
6F5
884
C2
R4
C3
R5
C4
R6
R9
VR 150/30
RELAY
R8
R7
C5
R10
6C5
6C5
6F6
927
R12
R14
R15
R16
R11
R17
R18
R19
R20
R13
R21
R22
R23
R24
927
R25
6F5
884
C7
R26
C6
R27
R28
R29
C8
C9
L1
To Filaments
T1
110 V A.C.
5Y4G

FIGURE 12

## ELECTRONIC CONTROL CIRCUIT

### TABLE NO. 2 - LEGEND FOR FIG. 12

| | | | | | |
|---|---|---|---|---|---|
| $R_1$ | = | 330,000 ohms | $R_{21}$ | = | 15,000 ohms |
| $R_2$ | = | 10,000 " | $R_{22}$ | = | 25,000 " |
| $R_3$ | = | 300 " | $R_{23}$ | = | 5,000 " |
| $R_4$ | = | 100,000 " | $R_{24}$ | = | 25,000 " |
| $R_5$ | = | 50,000 " | $R_{25}$ | = | 5,000,000 " |
| $R_6$ | = | 400,000 " | $R_{26}$ | = | 10,000 " |
| $R_7$ | = | 400,000 " | $R_{27}$ | = | 330,000 " |
| $R_8$ | = | 20,000 " | $R_{28}$ | = | 300 " |
| $R_9$ | = | 25,000 " | $R_{29}$ | = | 100,000 " |
| $R_{10}$ | = | 100,000 " | $C_1$ | = | .005 microfarads |
| $R_{11}$ | = | 100,000 " | $C_2$ | = | .03 " |
| $R_{12}$ | = | 5,000,000 " | $C_3$ | = | .01 " |
| $R_{13}$ | = | 15,000 " | $C_4$ | = | .000035 " |
| $R_{14}$ | = | 25,000 " | $C_5$ | = | .000035 " |
| $R_{15}$ | = | 5,000 " | $C_6$ | = | .005 " |
| $R_{16}$ | = | 25,000 " | $C_7$ | = | .03 " |
| $R_{17}$ | = | 20,000 " | $C_8$ | = | .01 " |
| $R_{18}$ | = | 100,000 " | $C_9$ | = | 24 " |
| $R_{19}$ | = | 100,000 " | $L_1$ | = | 30 henries |
| $R_{20}$ | = | 10,000 " | $T_1$ | = | Hammond type 275. |

of an 884 thyratron used as a saw-tooth generator[82], a 6F5 used as a bias amplifier, and a 927 photo-tube.

The relay, an Aminco "Supersensitive" Mercury Relay, is activated at 10 milliamperes, and releases when the current is reduced to below 2 milliamperes. The current is controlled by the bias on the 6F6, as this tube is in series with the relay. The bias may be either of two values as determined by the condition of the Eccles-Jordan circuit. This circuit has two stable conditions, in either of which one tube is conducting while the other is cut off. When the right hand 6C5 is cut off, the bias on the 6F6 allows the tube to conduct the necessary 10 milliamperes to close the relay. When this 6C5 is conducting, the relay current is reduced to below 2 milliamperes. The VR150/30 in the voltage divider permits a maximum change in grid bias, at the same time reducing the d.c. drop across the grid return resister.

The Eccles-Jordan circuit is altered from one stable condition to the other by applying negative pulses to the grid of the tube to be cut off. These pulses are formed by passing a saw-tooth wave from a standard type 884 sweep circuit through a differentiating circuit. In Fig.12, the upper 884 thyratron supplies negative pulses through the differentiating circuit, $C_3$ $R_{19}$, to the grid of the right 6C5, cutting it off and closing the relay. In a similar manner, the lower 884 functions to open the relay.

The saw-tooth wave is only produced when the bias on the thyratron is lifted to a point where the tube can "fire". This bias is controlled by a bridge circuit with a 6F5 forming a variable resistance element in one arm. When the light falls on the corresponding photo-cell, the negative voltage drop across the grid return resister of the 6F5 is increased, causing an increase in the resistance of this arm of the bridge, thus permitting the 884 to function. The 6F5 is a high gain tube, and care must be taken to prevent oscillation if the leads from the photo-cell are long. However, since this is a d.c. amplifier, it is permissible to use a large by-pass condenser from plate to ground.

(b) Itemized Description:

The 5Y4G tube is a full-wave rectifier, which delivers 320 volts d.c. to a series of voltage dividers connected in parallel across the output. These voltage dividers supply the correct operating voltages for the various electron tubes used.

When no light is shining on the upper 927 photo-cell of Fig.12, the voltage across it is the same as the potential drop across resistance $R_{13}$. When, however, light shines on this cell, the light sensitive surface emits electrons, i.e. the cell conducts, and the potential of the anode decreases (becomes less positive). As the grid of the upper 6F5 is tied to this anode, it likewise

becomes less positive, or more negative. This change in bias "cutts off" the 6F5. As this tube is no longer conducting, the potential at the 6F5 anode increases, in turn making the grid of the 884 thyratron more positive. This allows the 884 to become conducting. (If desired, this 6F5 may also be considered as one variable resistance arm of the bridge net work $R_1$, $R_{15}$, $R_{14}$, 6F5 with the 884 connected between two corners of the diamond.) The 884 tube is connected to act as a saw-tooth generator, condenser $C_2$ being charged through $R_4$ under a constant potential until the potential across $C_2$ rises sufficiently to cause the 884 to "fire", i.e. rapidly discharge $C_2$. The condenser then begins to charge again. The "firing" thus continues as long as the light is on that photo-cell. During the time of charging, the potential is increasing almost linearly, and then drops rapidly to zero on firing. This leads to the designation of a saw-tooth wave form.

This saw-tooth generator then feeds to a differentiating circuit, $C_3$ $R_{19}$, which converts the saw-tooth to a series of negative "pips"; each pip corresponds to one firing of the thyratron. At the firing of the 884, the potential on the left side of $C_3$, which was constant during charging, suddenly drops, causing a negative pulse to come from the right hand side of $C_3$. As the $C_2$ begins to charge again, $C_3$ resumes its previous constant potential, hence the term

"differentiating".

This negative pulse from $C_3$ makes the grid of the right hand 6C5 negative, preventing the tube from conducting. This, in turn, raises the potential of the anode of this tube. As this anode is connected to the grid of the left hand 6C5, that grid becomes more positive and the tube conducts.

At the same time, since the right hand 6C5 is cut off, the potential of the anode is raised. This supplies sufficient bias to the 6F6 (through the intermediate VR150/30) to allow that pentode to conduct and operate the relay.

When the light falls on the lower photo-cell, the pulses are similarly transmitted to the grid of the left hand 6C5, cutting it off. This, in turn, raises the potential of the right hand 6C5, which may now conduct. This, then results in the cutting off of the 6F6 and the accompanying release of the relay.

### 3. Auxiliary Apparatus:

The control itself was mounted on an 8 x 12" metal chassis, equipped with a toggle switch, 2 ampere fuse, pilot-light, etc. The connections to the relay and the photo-cells were through plug connectors. The leads to the photo-cells were of metal-sheathed cable, the sheath, as well as the chassis, being grounded.

The galvanometer, slit light source, and photo-cells, of Fig.11, were mounted in a wooden box. A scale drawing is shown in Fig.13. The galvanometer was a Leeds & Northrup Type 2400, sensitivity .003 microamperes per mm. at one metre. As the operating distance from photo-cells to galvanometer was approximately 5 feet, this resulted in a very sensitive arrangement. A Westinghouse Mazda #2330 automobile head light bulb was used to supply the light. It was operated on slightly less than 6 volts A.C. This light was so placed as to be at the focal point of a large convex collecting lens of focal length 3 cm. This lens had a slit opening, thus yielding a narrow beam of parallel light, which was reflected from the galvanometer mirror back to the photo-cells.

All parts inside the box were blackened with lamp black to cut down internal light reflection. A shielded opening was made in the lid above the light bulb for convection cooling.

The constant backing e.m.f. of Fig.11 was supplied by three 2-volt lead batteries in parallel (B) connected to a 200,000 ohm resistance (P) and a subdivided dial resistance box (R). The values of R could be varied as wished, to supply any e.m.f. desired for opposing the thermocouple e.m.f.

4. Operation:

Certain of the critical operating data of the control

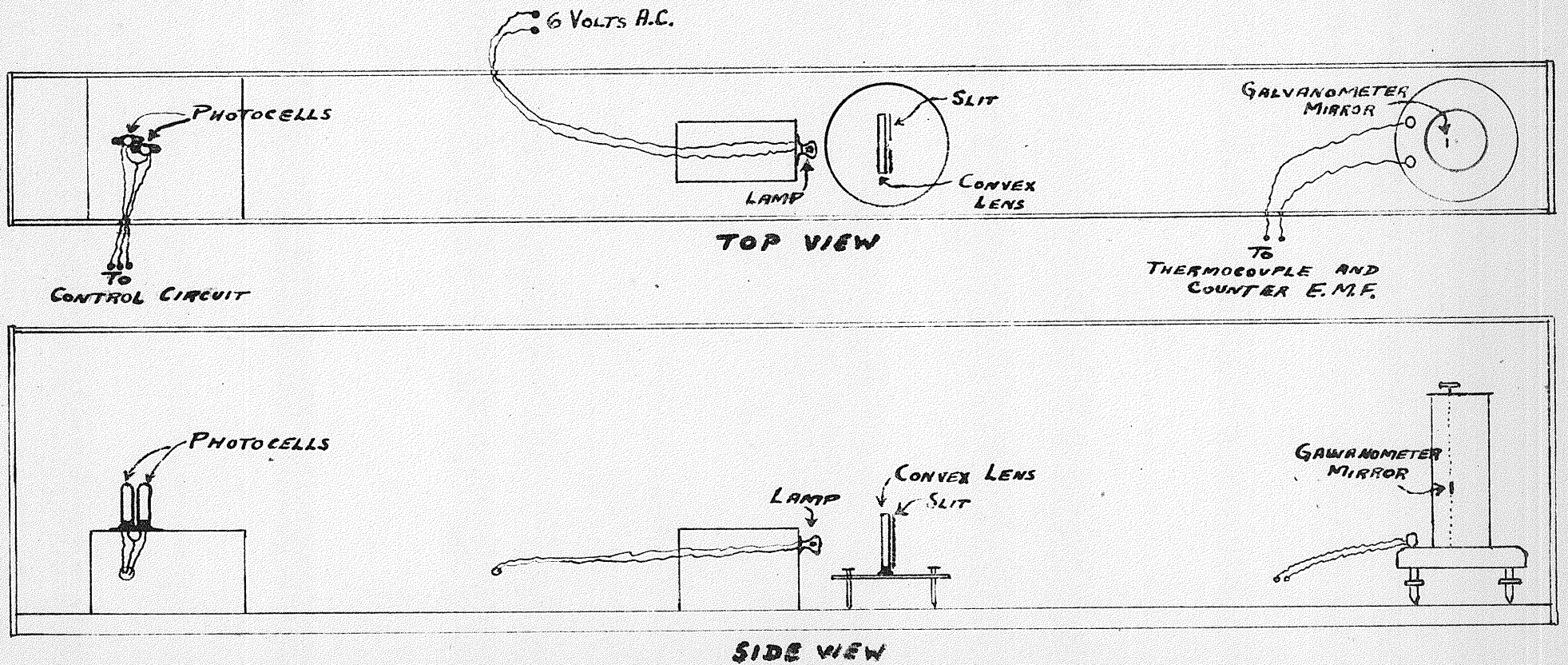
6 VOLTS A.C.
PHOTOCELLS
SLIT
CONVEX LENS
LAMP
GALVANOMETER MIRROR
TO CONTROL CIRCUIT
TO THERMOCOUPLE AND COUNTER E.M.F.
TOP VIEW
PHOTOCELLS
LAMP
CONVEX LENS
SLIT
GALVANOMETER MIRROR
SIDE VIEW
SCALE
1" = 6"
0 3 6 INCHES

FIGURE 13

circuit are given in Table 3 for reference in maintenance of the set.

TABLE NO. 3 - The Possible Critical Operating Voltages of the Electronic Control Circuit.

| Voltage across | | |
|---|---|---|
| $R_{20}$ | - | 320 volts |
| $R_{16}$ & $R_{24}$ | - | 126 " |
| $R_{15}$ & $R_{23}$ | - | 24 " |
| $R_{14}$ & $R_{22}$ | - | 122 " |
| $R_{13}$ & $R_{21}$ | - | 67 " |
| $R_4$ & $R_{29}$ | - | 0 volts when light off cell,<br>50 volts when light on cell. |
| $R_1$ & $R_{27}$ | - | 65 volts when light off cell,<br>15 to 20 volts when light on cell.<br>(must drop to below 40 volts to operate). |
| $R_{17}$ | - | 62 volts |
| Centre tap of $R_{20}$ to Ground | - | 72 volts. |

Very little difficulty was encountered in the maintenance of the circuit. During the initial tuning stage, many parts were functioning under considerable overload for up to five hundred hours. This time has not been reckoned in the time of operation. The 5Y4G was replaced after 1050 hours' service, and the two 927 photo-cells after 2200 hours. The circuit has had in excess of three thousand hours of thermostatting operation, having run as long as two weeks without being shut off, and the shut-downs were usually of

only a few hours duration.

It was found necessary, due to interference from the control outfit, to shield the leads from the thermocouple to the galvanometer in grounded metal casing where close to the set.

Mention should be made here of the present operating condition of the control circuit relay. It is to be noted from Fig.12 that the points of the electronic circuit to which the relay is connected are at about 320 volts above ground potential. Fig.14 shows the actual wiring of the relay. It is immediately obvious that, since the battery booster supplying the necessary 6 volts d.c. to the relay has a common terminal with the electronic control, a possible danger exists for a worker not familiar with the circuit. Accordingly, as the circuit will remain in operation, it is suggested that the wires marked with X's be removed and replaced with those represented by dotted lines. In this way, the battery booster will be entirely independent of the control circuit voltage, and no potential hazard will exist.

B. Other Apparatus:

The complete wiring diagram was as shown in Fig.15. The furnace and surroundings were the same as for the work on thermal analysis, thus providing the constant

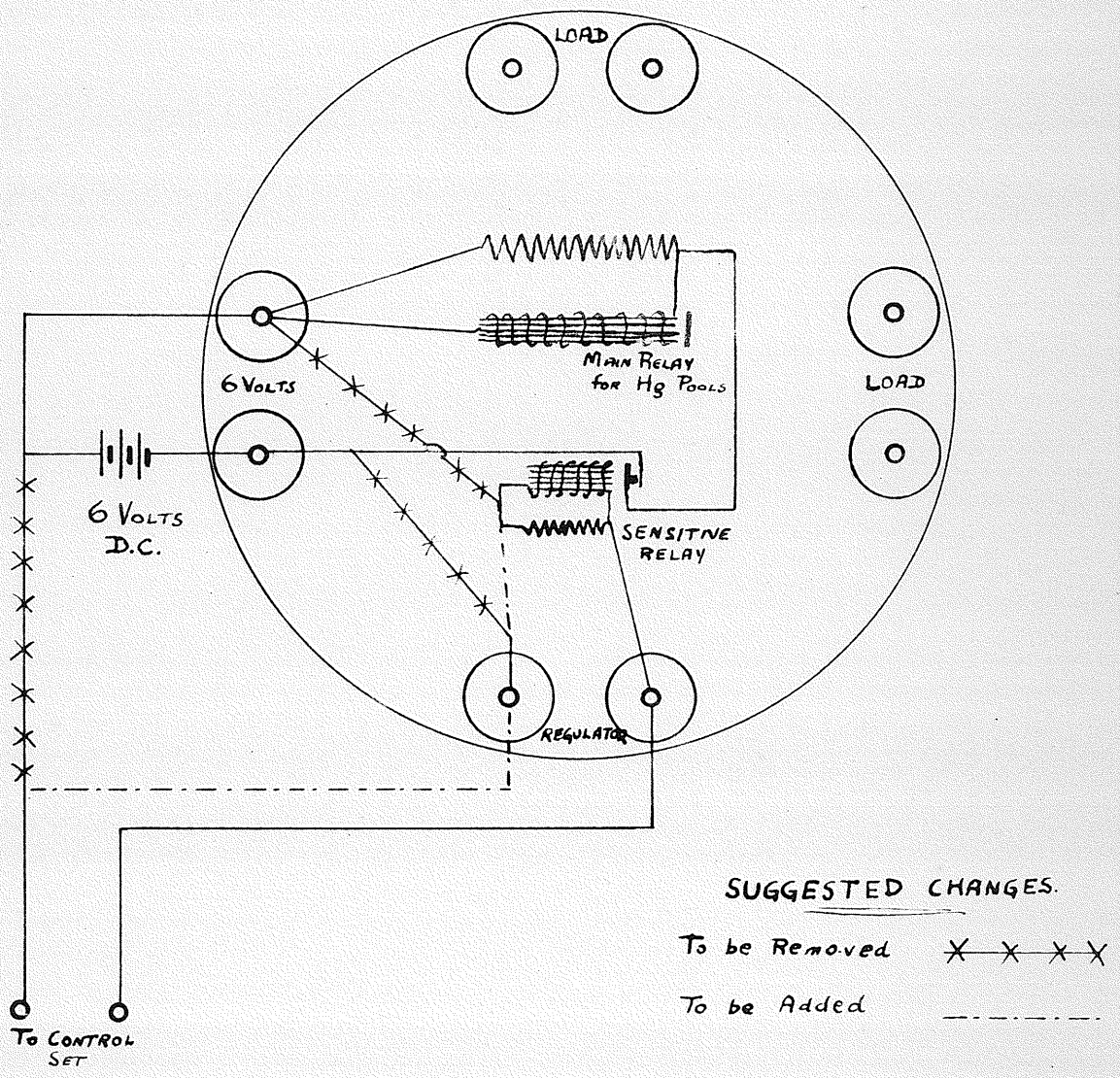
LOAD
6 VOLTS
MAIN RELAY FOR Hg POOLS
LOAD
6 VOLTS D.C.
SENSITIVE RELAY
REGULATOR
TO CONTROL SET
SUGGESTED CHANGES.
To be Removed
To be Added

FIGURE 14

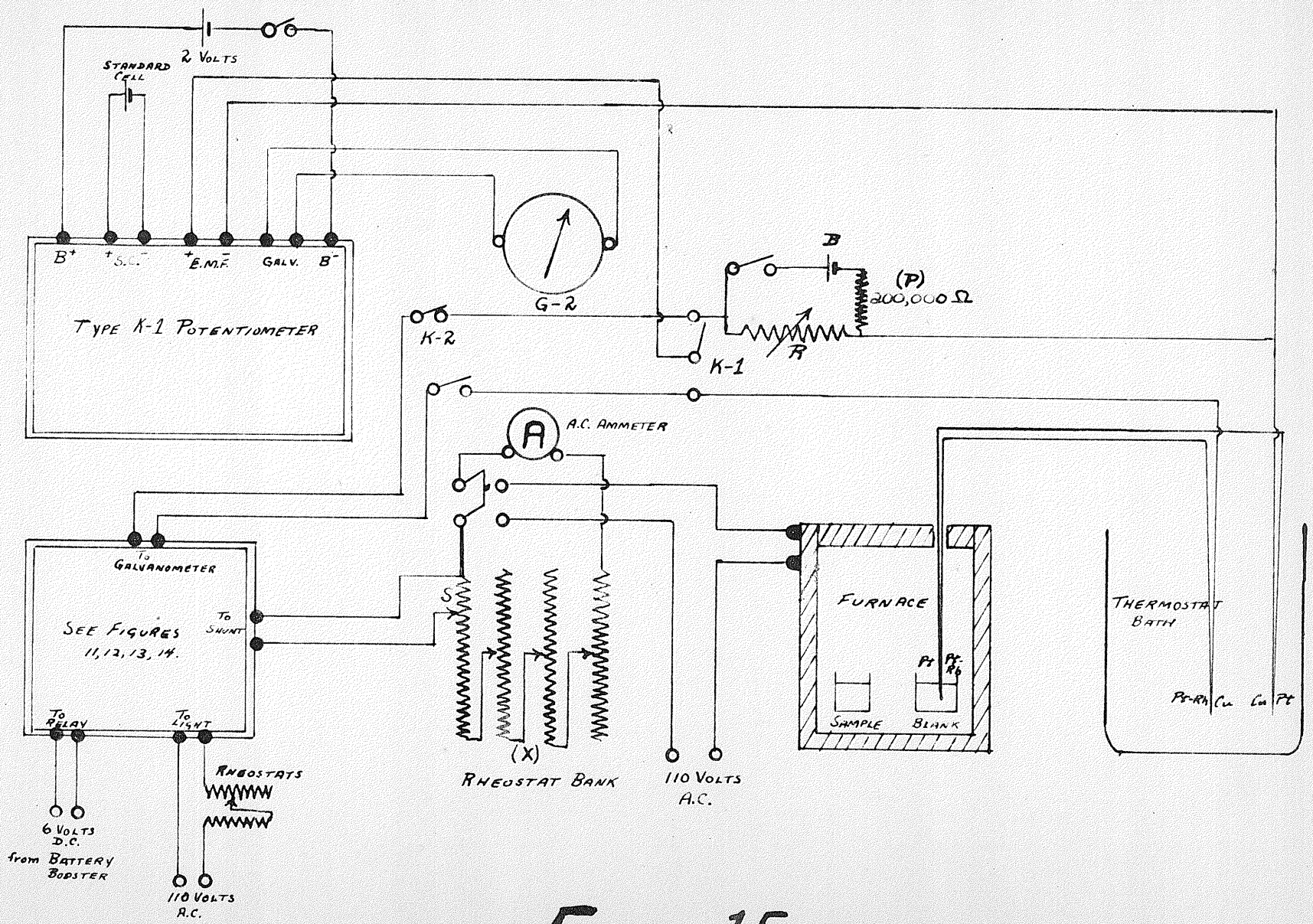
2 Volts
Standard Cell
B+ + S.C. − + E.M.F. − Galv. B−
Type K-1 Potentiometer
G-2
K-2
K-1
B
(P)
200,000 Ω
R
A
A.C. Ammeter
To Galvanometer
See Figures 11, 12, 13, 14.
To Shunt
To Relay
To Light
Rheostats
6 Volts D.C. from Battery Booster
110 Volts A.C.
S
(X)
Rheostat Bank
110 Volts A.C.
Furnace
Pt
Pt-Rh
Sample
Blank
Thermostat Bath
Pt-Rh Cu Cu Pt

FIGURE 15

temperature environment which is essential for isothermal work. Since it was necessary to thermostat the furnace for prolonged periods of time, as long as 10 days, it was necessary to use a thermostat for the cold junctions of the thermocouple. This thermostat was maintained at 31.7°C.

The switch K-1 of Fig.15 allowed the determination (with K-2 open) of either the controlling e.m.f. from the batteries or the voltage from the thermocouple.

Plate 1 gives a general view of the complete experimental setup. To the extreme left are the rheostats controlling the voltage to the automobile head-light bulb of the control outfit. Next is the shielded photo-cell box of Fig.13. Between this and the potentiometer is the control outfit mounted on a metal chassis. To the left of the furnace, with its constant temperature environment, lies the thermostat bath for the cold junctions of the thermocouple. In the immediate foreground is a refrigerator used for the quenching of samples.

Plates 2, 3 and 4 give a closeup view of the apparatus. Plate 3 clearly shows the grounded coaxial cable used for the connection of the photo-cells to the control circuit. Immediately in front of the chassis, the grounded shield used for the galvanometer leads may be seen. To the right of the control set is a relay that was used in the

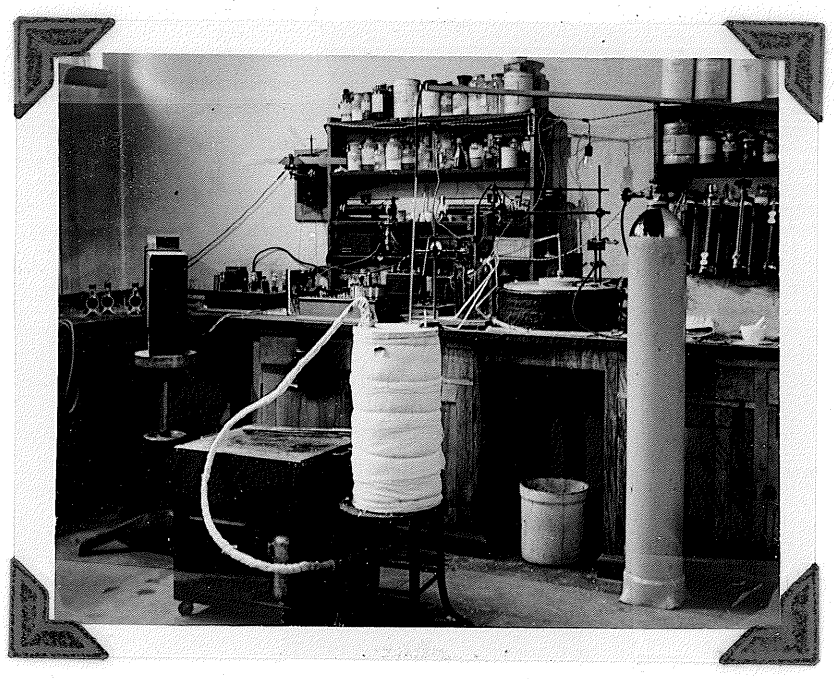

PLATE I.

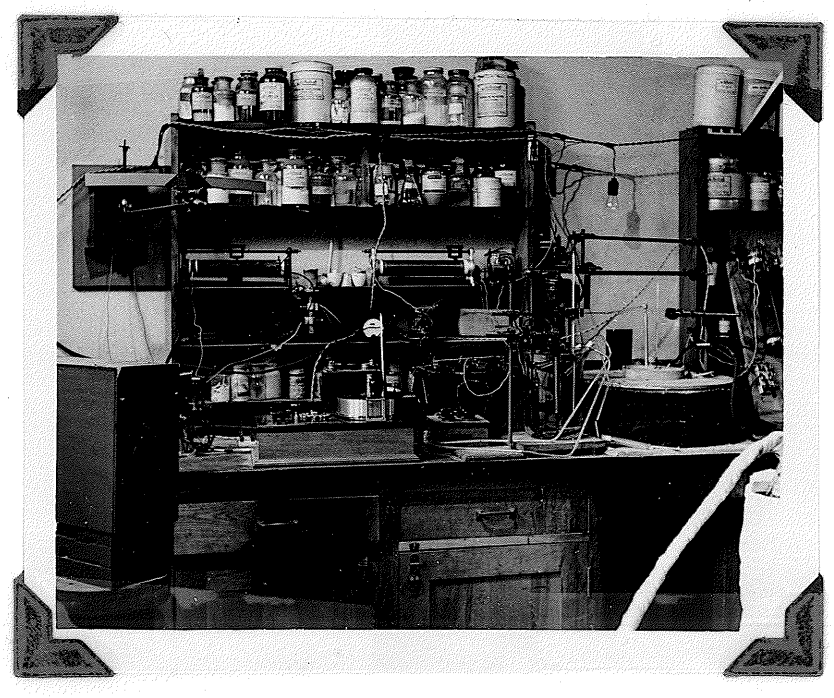

PLATE II.

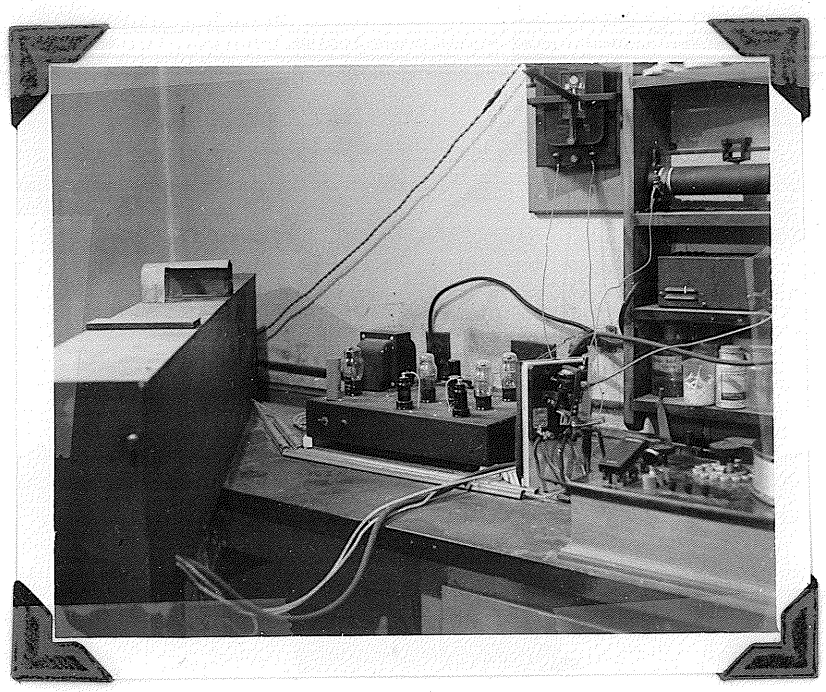

PLATE III.

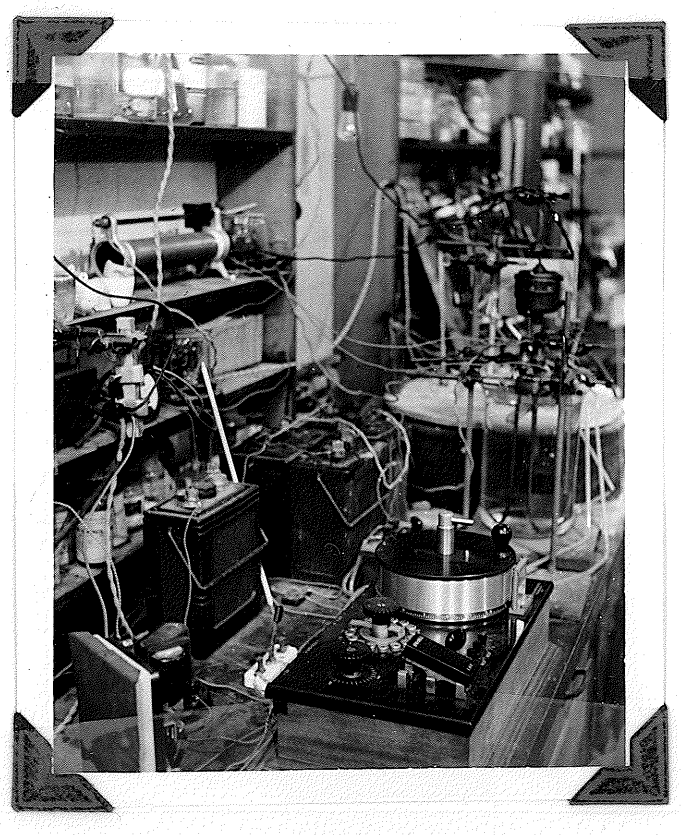

PLATE IV.

later stages of the work in place of key K-2 of Fig.15. This relay opened in the event of a power failure during the night, thus protecting the galvanometer. It was installed because of the frequent severe electrical storms which prevailed in this locality during July and August.

C. Procedure:

Initially, the samples were placed in Salamander Graphite Crucibles, and were covered with powdered graphite to prevent oxidation. A tin sample was usually from 250 to 300 grams and contained 3 grams of freshly polished fine Merck iron wire. The latter was wedged into the bottom half of the crucible before the molten tin was poured onto it. If the wire was not wedged in the bottom, the entrapped air would make it float to the surface. The sample was immediately covered with powdered graphite and placed in the furnace. The thermocouple case was then placed directly in the melt. The sample, thus prepared, was heated to between 700° and 800°C. for five hours, after which it was thermostatted at the desired temperature for several days. Since fine wire was used, all the iron added in excess of the solubility limit reacted, on heating, with the tin to form, at the bottom of the crucible, the stable solid phase for that temperature region.

Several attempts were made to pipette molten analysis samples from the top part, using various filter arrangements. However, the protective charcoal layer on top of the sample prevented this.

As a result, it was decided that the only alternative lay in quenching the sample, hack-sawing it down the centre, and taking drill samples from the top half. All analyses in this, and the succeeding work, were done colormetrically (see page 34). Samples obtained in this manner gave no consistent results. Moreover, a polished and etched cross-section of one such sample showed no marked tendency of excess solid phase to settle (presumably due to the closeness of the density of the solid phase to that of liquid tin). Using the values of Ehret & Westgren[50], the calculated densities of solid phases are

| | | |
|---|---|---|
| $FeSn_2$ | 7.31 | g/cc. |
| FeSn | 7.54 | " |

The density of molten tin[83] is

| | | |
|---|---|---|
| 6.87 | at | 400°C. |
| 6.81 | " | 500 |
| 6.76 | " | 600 |
| 6.69 | " | 700 |
| 6.64 | " | 800 |
| 6.59 | " | 900 |

As is immediately apparent, the difference in density is not great. Probably, with sufficient time, settlement would have been complete. However, time was an important factor in the investigation; accordingly further work along this line could not be pursued.

The following method was found to give very satisfactory results up to 600°C. The graphite crucible was lined with alundum powder in the form of a water paste. This, on drying, gave a very sturdy crucible that could not contaminate the samples with carbon. The iron was added as before in the form of fine Merck wire, the tin being poured in after the polished wire was wedged at the bottom of the cricible. The sample was then immediately covered with very fine magnesia powder. The samples prepared in this way were placed in the furnace, the thermocouple case was inserted in the melt, and the furnace was brought up to the desired temperature and maintained there. A considerable variation in the time of thermostatting was used. Thus, if all points fell on a smooth curve, a better guarantee of equilibrium was obtained. This would not have been necessary if the previous method had proven suitable, thus allowing equilibrium to be approached from both sides. At the end of the required period, the sample was quickly removed from the furnace and quenched. In view of the previously observed slowness of settling for suspended solid phase, there was no need for the rapid quenching required for microscopic or X-ray samples. All samples were, however, cold within three to five minutes of removal from the furnace.

The quenched samples readily fell from the crucible,

thus eliminating the necessity of smashing the crucible.

The samples were cut down the centre, and drillings taken from a horizontal row as close to the top as possible. Separate drillings were also made from another row just below the first. Check results on the above two samples were obtained up to 550°C.

It should be noted that at the lower temperatures the solubility of the iron compound in tin was such that with an ordinary soft steel drill bit an appreciable amount of iron was added from the bit. The soft steel drills would lose .0001 to .00015 grams weight while obtaining one such sample. Now, .00015 gm. in 15 grams of sample corresponds to .001% Fe. The solubility of iron compound in tin at 330°C. was found to be only .007%. Accordingly, all drillings were taken with a high speed tungsten steel bit. Even this lost about .00005 grams weight during each drilling.

One determination was made at 270°C. by placing the sample in an ordinary muffle furnace for 3-1/2 weeks. The temperature control here was no better than $\pm$ 15°C. but this was unimportant due to the steepness of the liquidus in this region.

For temperatures above 600°C. there appeared a marked discrepancy in iron content between the two rows of drillings, the upper layer giving a lower assay. Moreover, some scoria was formed on the furface with these samples. No improvement was obtained by using molten salt layers

as a surface protection. An analysis of 3 grams of this scoria gave over 66% Fe, or about 85% FeO. Thus, it was apparent that the iron was being preferentially burnt out of the alloy.

Filling the furnace with nitrogen (99.8%) directly from a commercial cylinder without further purification, and allowing a slow stream to flow through the furnace during the period of thermostatting, did nothing to improve this trouble.

In an attempt to prevent this oxidation, polished iron wire was placed at the bottom of a standard 8xl inch Pyrex test tube and the required amount of molten tin was poured in (about 100 grams). Usually about 2 grams of fine Merck wire (about 30 feet) and 6 to 10 grams of Cenco wire (about 6 pieces) were used. The sample was then put under vacuum using a water pump, heated, and gently tapped to liberate the many large air bubbles trapped in the wire. The tin was then allowed to solidify while still under vacuum. When cold, the tube was sealed under high vacuum, the seal being made as close to the metal surface as possible. The glass capsule so formed was placed in a crucible and was supported by alundum powder so that the shape of the capsule would not change while in the furnace. Very clean samples were obtained in this way, the only scoria present being that formed while the sample was heated to remove entrapped air.

Drillings were taken from the top part of the quenched sample by drilling straight through without first cutting longitudinally. The liquidus was investigated from 600° to 900°C. in this manner.

For these samples in sealed glass capsules, the temperatures determined were those of another sample of tin so situated in the furnace that both would be at the same temperature.

Since the furnace was circular, and had the heating element wound uniformly about it, there is little danger that symmetrically placed samples did not acquire the same temperatures.

All analyses for the glass protected samples were run colormetrically; check results were obtained using the volumetric method described on page 36.

# RESULTS

## RESULTS

### I. The Determination of the Eutectic Composition:

Using equation 2 (page 6), namely

$$\triangle T_f = \frac{RT_o^2 M_1 m}{1000\, L_f}$$

where R = 1.987 cal/mole,

$L_f$ = 1660 cal/mole,

the calculated difference in the freezing point of spectroscopic tin and absolutely pure Sn is

| | | |
|---|---|---|
| Pb | $\triangle T_f$ = | .0009°C. |
| Cu | = | .0028 |
| Fe | = | .0105 |
| As | = | .0005 |
| | $\triangle T_f$ = | .015°C. |

It is apparent from the above that 2/3 of the freezing point depression for spectroscopic tin is due to its iron content.

In work with the Beckmann thermometer, constancy of freezing point was obtained to within .002°C. However, because of the difficulty in obtaining constancy in thermometer settings, it is doubtful if better than .01°C. can be claimed. This, then, would set the eutectic value at less than .003% Fe.

On page 43, it was mentioned that a trial with the Pt - PtRh thermocouple was made on pure tin and iron-rich tin in order to determine whether any difference could be

detected. No difference was detectible, but this method was by no means as sensitive as the Beckmann results. However, it did guarantee that the eutectic depression was less than .1°C. corresponding to less than .015% Fe present in the eutectic.

Work on the isothermal study gave a very accurate measure of the eutectic composition. At 329°C. the solubility of iron compound in liquid tin was found to be .0073% Fe, while at 270°C. it was .0046%. Joining these two points by a straight line gives a value on extrapolation of .0030 ± .0010% Fe at 232°C.

In view of the extreme steepness of the curve, this extrapolation is quite justifiable. Actually a value obtained in this way would tend to be low rather than high because of the slight curvature that must be present in the liquidus line.

II. Thermal Analysis:

A typical plot on a very reduced scale, and showing only every tenth point, is given in Fig.16. This graph is for tin containing .056% Fe. A plot (not shown here) was also made, on a very expanded scale, of the change in galvanometer scale readings per minute against the temperature of the sample, i.e. $\frac{\triangle L}{\triangle t}$ vs $\theta$, where L is the scale reading of the galvanometer. This is a fairly sensitive plot, and corresponds to Fig.3(d) with the axes interchanged.

No break in the cooling rate could be detected on this curve. Likewise, no break was observed for the two higher iron additions, .5% and 3%, which were studied in this manner.

An analysis of the tin, later, showed this was an actual iron content of less than 2%.

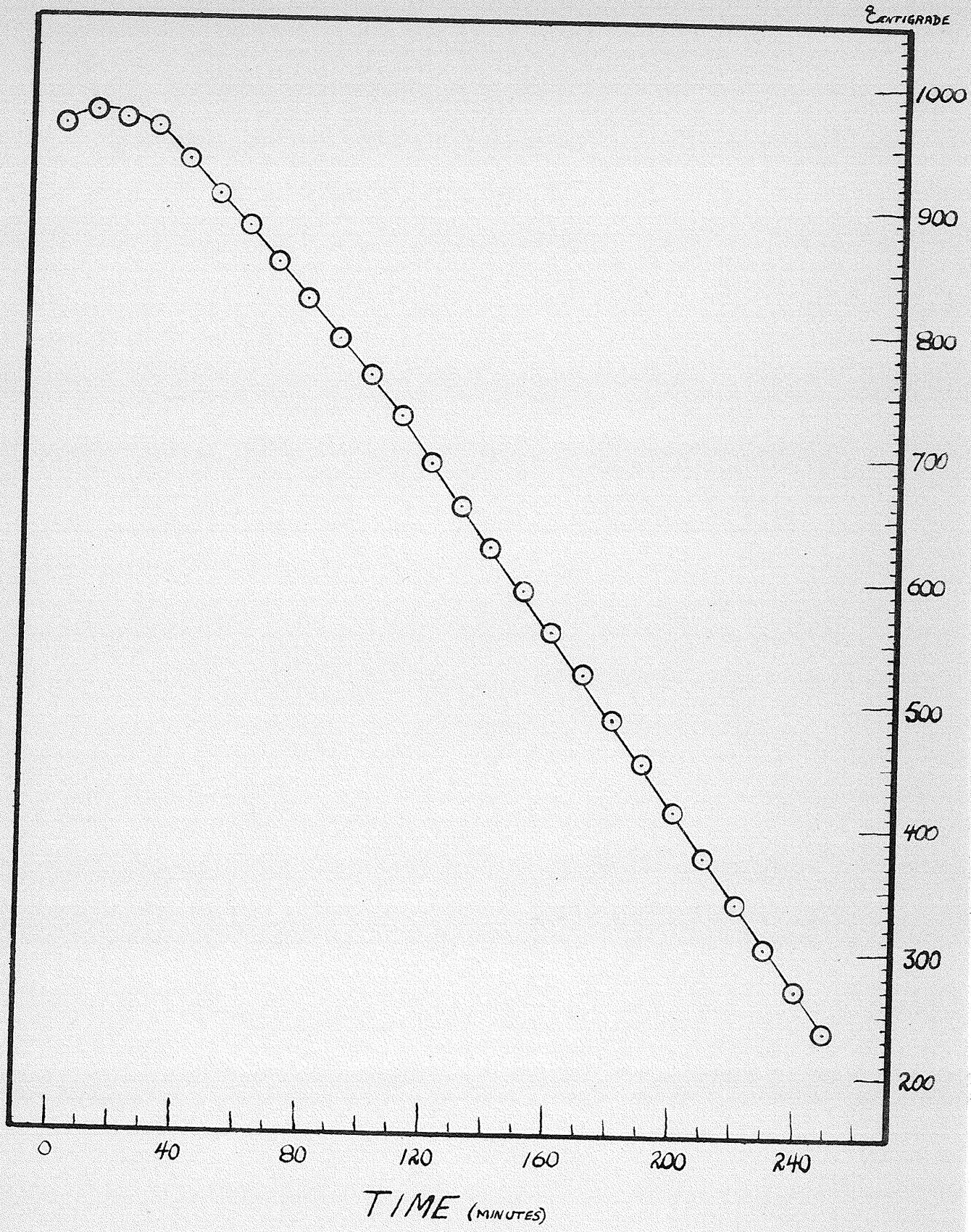
°CENTIGRADE
1000
900
800
700
600
500
400
300
200
0
40
80
120
160
200
240
TIME (MINUTES)

FIGURE 16

III. Isothermal Analysis:

All the results listed below are for samples which were not preheated prior to being thermostatted.

TABLE 4 - Iron Content of Samples Protected by Magnesia Covering.

| No. | Temperature | Time of Thermostatting | % Fe |
|---|---|---|---|
| 1 | 270°C. | 25 days | .0047 |
| 2 | 329 | 10 " | .0073 |
| 3 | 382 | 3 " | .023 |
| 4 | 389 | 6 " | .029 |
| 5 | 394 | 2 " | .022 |
| 6 | 426 | 5 " | .022 |
| 7 | 451 | 2 " | .046 |
| 8 | 454 | 5 " | .043 |
| 9 | 483 | 7 " | .070 |
| 10 | 502 | 5½ " | .087 |
| 11 | 548 | 3 " | .141 |
| 12 | 576 | 5 " | .169 |
| 13 | 594 | 2 " | .222 |
| 14 | 606 | 5 " | .221 |
| 15 | 654 | 3 " | .32 |

TABLE 5 - Iron Content of Samples Sealed under Vacuum in Glass.

| No. | Temperature | Time of Thermostatting | % Fe |
|---|---|---|---|
| 16 | 637°C. | 2 days | .322 |
| 17 | 700 | 1 " | .75 |
| 18 | 746 | 2 " | .96 |
| 19 | 774 | 1 " | 1.59 |
| 20 | 801 | 1 " | 1.61 |
| 21 | 826 | 1 " | 1.72 |
| 22 | 846 | 1 " | 2.02 |
| 23 | 857 | 1 " | 2.11 |
| 24 | 895 | 1 " | 2.73 |

The above results are plotted in Fig.17 and Fig.18. Fig.17 shows the whole range of the liquidus studied. Fig.18 is a greatly enlarged view of a small section from 0 to .35% iron.

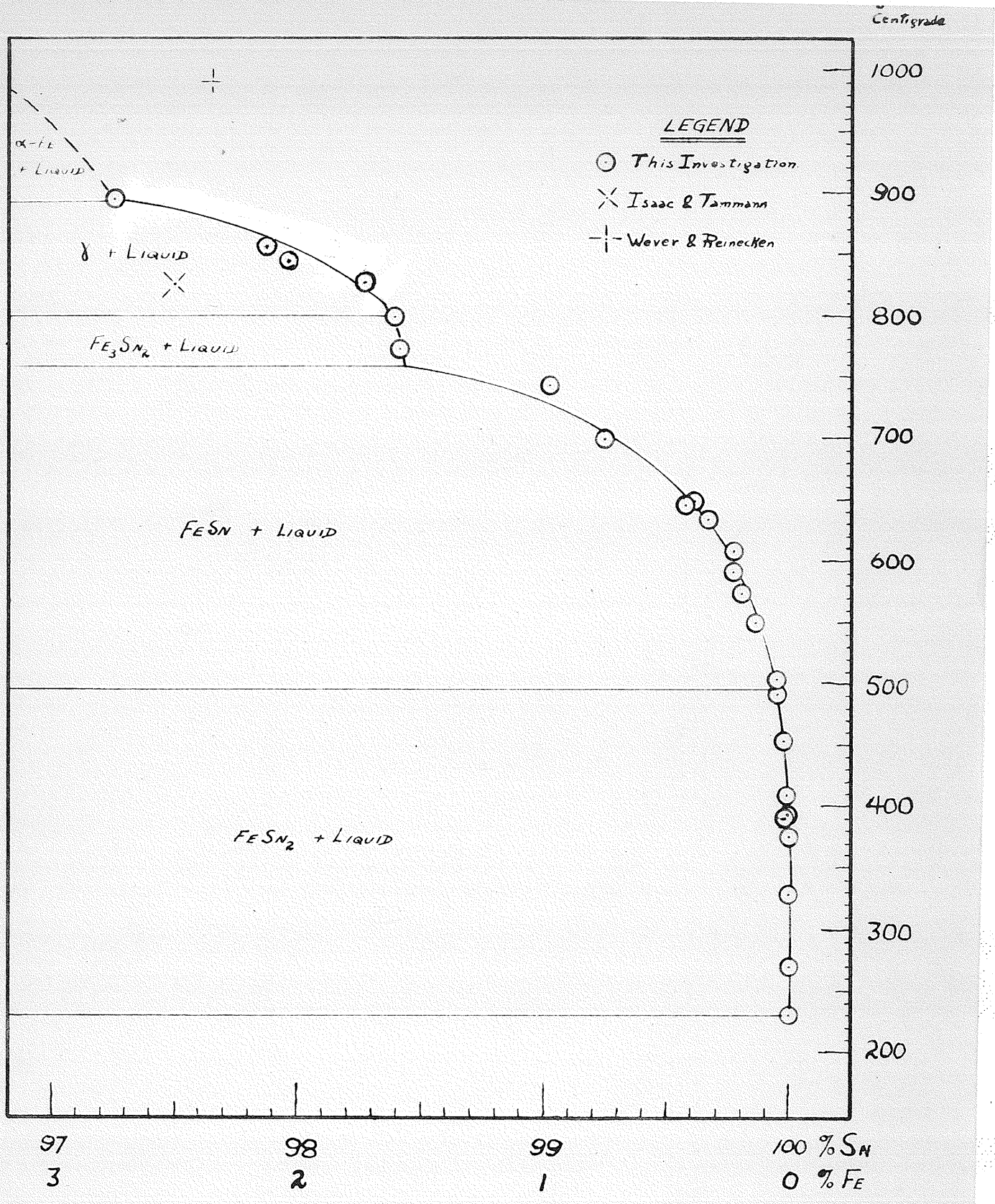


FIGURE 17 THE LIQUIDUS OF IRON-TIN
(HIGH TIN END)

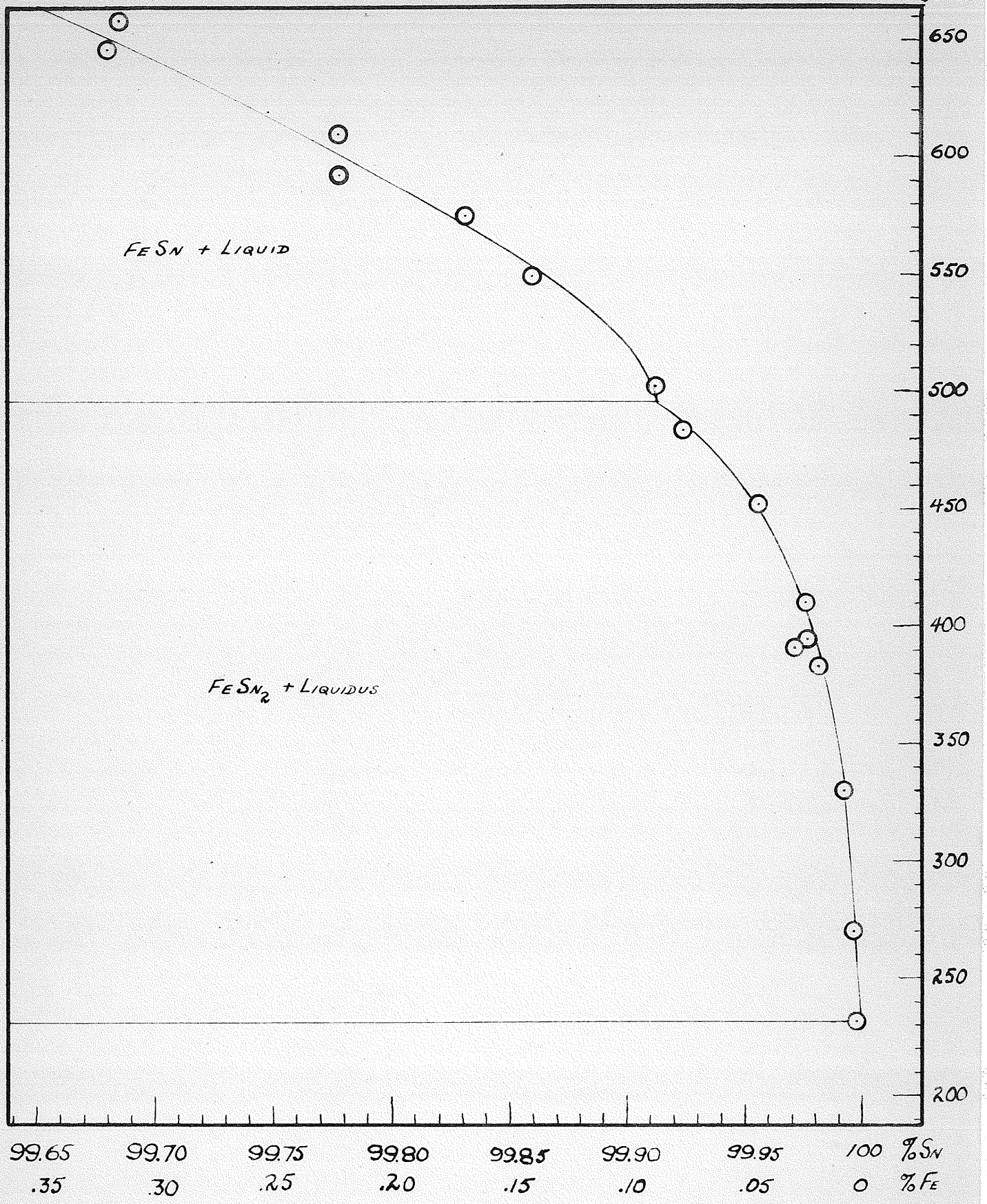


FIGURE 18 THE LIQUIDUS OF IRON-TIN
(VERY HIGH TIN END)

It was mentioned earlier that from 550°C. upwards the total free iron content at the end of the run was very much lower than the amount originally added. Below are listed the results obtained in samples that were afterwards rejected when it was realized that oxidation had occurred. Along with these are listed the values obtained from Fig.17 for the solubilities at the same temperatures.

TABLE 6 - Iron Content of Samples Subject to Oxidation.

| No. | Temperature | % Fe | |
|---|---|---|---|
| | | Found | from Graph |
| 1 | 699°C. | .39 | .71 |
| 2 | 703 | .092 | .73 |
| 3 | 751 | .200 | 1.38 |
| 4 | 770 | .38 | 1.58 |
| 5 | 796 | .21 | 1.61 |
| 6 | 808 | .36 | 1.62 |
| 7 | 858 | .26 | 2.09 |
| 8 | 872 | .38 | 2.25 |
| 9 | 894 | .32 | 2.73 |
| 10 | 934 | .185 | 3 |

# DISCUSSION OF RESULTS

## DISCUSSION OF RESULTS

The value of the eutectic composition, found by straight line extrapolation of the solubility figures at 270° and 329°C. was .0030 ± .0010% Fe. This is in very good agreement with the limits set by the use of the Beckmann thermometer. The possible error of ± .0010% is determined as a maximum error possible in extrapolation due to possible errors in the temperature readings and the analyses.

In view of the very low iron content of the eutectic, it is not surprising that no previous investigations have been reported. It is unlikely that any results will ever be obtainable on the solid solubility of Fe in Sn.

On page 29, there is a quotation from a paper by Hanson, Sandford & Stevens[27] stating that the freezing point of tin varied considerably with the iron content. In view of the above determination of the eutectic composition, it would appear that this statement was made rather carelessly.

It is interesting to note that, assuming the eutectic to be .0030%, the best tin available (the Vulcan Spectroscopic Tin) containing .0015% Fe, and the next best .002%, show very little purification over this figure.

It is difficult to understand why the Roberts-Austen method of thermal analysis did not prove at least partially successful for the high iron content. Probably a slower rate of cooling would have achieved the desired result. The difference in total iron added to the sample, namely 3%, and the final iron content, less than 2%, is probably due to oxidation of the reduced iron before it was able to come into actual contact with the tin.

The electronic control circuit proved very satisfactory in the isothermal investigation. It was found that samples could be thermostatted indefinitely to within $\pm$ 3°C. of the desired temperature. However, the geometry of the optical system could be improved slightly, if required, in order to increase the accuracy of thermostatting. For work in this and higher temperature ranges, it is very unlikely that more accurate control will be needed.

Including the possible errors in the actual determination of the temperature of the samples, it is felt that all temperatures reported are correct to within $\pm$ 5°C.

It will be noted that in the isothermal determinations, there was a considerable variation in the time of

thermostatting. As all the points lay in a good line, it would appear that at 400°C. two days were more than ample time for equilibrium to be attained. However, the use of longer periods of time for many trials serves as a definite proof that equilibrium had been reached. This was the only proof that could be used in view of the difficulty in approaching equilibrium from supersaturation.

The results for the samples sealed in glass capsules coincided with, and overlapped, the results obtained with the first samples protected only by magnesia. Thus, it was apparent that one day was more than ample for the attaining of equilibrium at temperatures above 600°C.

There appears to be a definite, though not marked, break in the liquidus curve at 496°C. (Fig.18). This coincides with the transition from $FeSn_2$ to FeSn. The experimental points appear to show another definite break in the region of 755°C. According to the X-ray study of Ehret & Gurinsky[51] this would correspond to the phase change from FeSn to $Fe_3Sn_2$. It is interesting to note that Wever & Reinecken[56] had reported a thermal arrest point at 755°C. for this concentration region, but that Edwards & Preece[49] had later decided against it. The break at 800°C. in the liquidus for the

transition from $Fe_3Sn_2$ to $\gamma$ is not so marked. Time did not allow the work to be carried to 1000°C. as originally planned, but presumably another break should be observable at 890°C.

G.B.Skinner[69], working downwards from the region of immiscibility, should be able to complete the curve and, at the same time, give an independent check on the upper portion of the curve as shown in Fig.17.

Early in the investigation, it was suspected that some of the previously mentioned data obtained at Trail on the solubility of iron compounds in tin were low. This was confirmed when the final values for the liquidus were determined. It is felt that this difference is due to the aeration that must occur during the plant operations, especially filtering, and during any pilot tests of a similar nature in the laboratory.

The data of Table 6 prove beyond question that iron is burnt preferentially from tin at the higher temperatures, even with only slight contact with air. It is not surprising, then, that the Fe assays in the tin smelted at Kimberley are low. Jones & Thunaes[4] stated that aeration occurs during "the passage of crude tin down the 10 foot launder and its fall of 2 to 4 feet from the end of the launder into the pot." Moreover, what is of even more importance, compressed

air is used in their filtration process, and this would also favor oxidation. The Trail results were, however, of the correct order of magnitude.

Accordingly, the primary purpose of this investigation, namely the determination as to why the results of the Consolidated Mining and Smelting Company Limited for the solubility of iron compounds in tin do not agree with those of the previously published literature, has been accomplished.

First of all, this literature showed solubility that was far too high; and, secondly, the plant procedure at Trail yields results which are lower than would be expected.

# SUMMARY

## SUMMARY

1. A control circuit was designed for use in isothermal investigation. It permits the thermostatting of any wire-resistance furnace for temperatures up to at least 2000°C. Used with a Pt - Pt 10%Rh thermocouple, the furnace may be maintained to within ± 5°C. of any desired temperature.

2. The eutectic composition of iron in tin has been determined as .0030 ± .0010% Fe.

3. The solubility of the iron compounds in liquid tin, the liquidus curve, has been determined from the melting point of tin at 232°C. through to 900°C. (See Figs. 17 and 18).

4. It has been found that iron is preferentially burnt from tin, and this is suggested as an explanation of the low values of some of the solubility data obtained in plant operations at the Kimberley Tin Smelter.

# BIBLIOGRAPHY

## BIBLIOGRAPHY


1. E.Isaac & G.Tammann, Zeit. anorg. Chem. 53 281 (1907)

2. W.G.Jones & W.E.Hoare, Jour. Iron Steel Inst. 129i 273 (1934)

3. O.E.Rommig, Metal Prog. 42 899 (1942)

4. E.J.Jones & A.Thunaes, Trans. Can. Inst. Min. Met. 47 35 (1944)

5. C.H.Wright, Private Comm.

6. C.H.Wright, ibid.

7. W.Gibbs, Trans. Conn. Acad. Sci. (1876-8)

8. H.von Jüptner von Johnstorff, Stahl u. Eisen, 55 666 (1899)

9. H.LeChatelier, Compt. rend. 130 85 (1900)

10. W.H.B.Roozeboom, Zeit. physik. Chem. 28 494 (1899), 30 385 (1899).

11. G.N.Lewis & M.Randall, Thermodynamics and the Free Energy of Chemical Substances (McGraw-Hill) 1st Ed. 1923, p.158.

12. H.Lipson & A.J.C.Wilson, Jour. Iron Steel Inst. 142ii 107 (1940)

13. F.H.Getman & F.Daniels, Outlines of Physical Chemistry (John Wiley) 7th Ed. 1943, p.210.

14. C.H.Heycock & F.H.Neville, J. Chem. Soc. 57 376, 656 (1890)

15. G.N.Lewis & M.Randall, Loc. cit. p.198.

16. C.H.Heycock & F.H.Neville, J. Chem. Soc. 61 888 (1892)

17. G.K.Burgess, Bull. Bur. Stds. 5 199 (1908-9)

18. W.Rosenhain, Proc. Phys. Soc. 21 180 (1908)

19. - Frankenheim, Pogg. Ann. der Physik, 37 38 (1836-7)

20. W.Plato, Zeit. physik. Chem. 55 721 (1906)

21. W.C.Roberts-Austen, Proc. Inst. Mech. Engrs. 35 (1899)

22. - Saladin, Iron Steel Metallurgy & Metallography, 7 237 (1904)

23. H.M.Howe, Trans. Emer. Min. Engrs. 23 466 (1893)

24. C.H.Heycock & F.H.Neville, Phil. Trans. 202A 1 (1902)

25. H.J.Miller, J. Inst. Metals, 37 188 (1927)

26. W.L.Fink, K.R.van Horn, & P.M.Budge, Trans. Amer. Inst. Min. Met. Engrs. - Inst. Metals Div. 93 421 (1931)

27. D.Hanson, E.J.Sandford, & H.Stevens, J. Inst. Metals, 55 341 (1934)

28. R.K.Waring, E.A.Anderson, R.D.Springer, & R.L.Wilcox, Trans. Amer. Inst. Min. Met. Engrs. 111 254 (1934)

29. C.H.Desch, Metallography (Longsman-Green) 5th Ed. 1942, p.2.

30. C.H.Desch, ibid, p.133.

31. R.W.G.Wyckoff, The Structure of Crystals, A.C.S. Monograph No.19 (Rheinhold) 2nd Ed. 1931, Supp. 1935.

32. G.L.Clark, Applied X-rays (McGraw-Hill) 3rd Ed. 1940.

33. W.P.Davey, Study of Crystal Structure And Its Application, (McGraw-Hill) 1st Ed. 1934.

34. A.F.Westgren, Trans. Amer. Inst. Min. Met. Engrs. - Inst. Metals Div. 93 13 (1931)

35. A.J. Bradley, H.J.Goldsmith, H.Lipson, & E.A.Taylor, Nature, 140 543 (1937)

36. W.Hume-Rothery & P.W.Reynolds, Proc. Roy. Soc. 167A 25 (1938)

37. A.Matthiesen, Brit. Assoc. Rep. 37 (1863)

38. J.H.van't Hoff & - van Deventer, Z. Physik. Chem. 1 185 (1887)

39. C.H.Desch & B.S.Smith, J. Iron & Steel Inst. 122i 358 (1929)

40. C.W.Waidner & G.K.Burgess, Bull. Bur. Stds. 7 1 (1911)

41. J.H.Adams & J.Johnston, Am. J. Sci. 33 534 (1912)

42. L.Holborn & F.Henning, Bur. Stds. Cir.No.66 (1917)

43. C.H.M.Jenkins & M.L.V.Gayler, Proc. Roy. Soc. 129A 91 (1930)

44. J.Chipman & S.Marshall, J.A.C.S. 62 299 (1940)

45. A.P.Wangsgard, Phy. Rev. 57 559 (1940)

46. - Lassaigne, Jour. chim. med. 6 609 (1830)

47. H.S.Deville & H.Caron, Compt. rend. 46 764 (1858)

48. W.P.Headden, Am. J. Sci. 144 464 (1892)

49. C.A.Edwards & A.Preece, J. Iron Steel Inst. 124ii 41 (1931)

50. W.F.Ehret & A.F,Westgren, J.A.C.S. 55 1339 (1933)

51. W.F.Ehret & D.H.Gurinsky, J.A.C.S. 65 1226 (1943)

52. C.Nöllner, Annalen, 115 233 (1860)

53. P.Pingault, Comp. rend. 199 1223 (1934)

54. H.J.Wollbaum, Z. Metallkunde, 35 218 (1943)

55. H.Nowotny & K.Schubert, Naturwissenschaften, 31 592 (1943)

56. F.Wever & W.Reinecken, Zeit. anorg. allg. Chem. 151 349 (1926)

57. L.J.Spencer, Mineral. Mag. & Jour. Mineral. Soc. 19 113 (1921)

58. C.Rammelsberg, Pogg. Ann. der Physik. 120 55 (1863)

59. A.S.Russell, T.R.Kennedy, J.Howitt, & H.A.M.Lyons, J. Chem. Soc. 1932 2340.

60. O.Nial, Arkiv. Kemi, Minerol. Geol. 17B No.11 (1943)

61. - Berthier, Jahresbericht u. die Fortschitte der Chem. 239 (1863)

62. - Bergmann, Gmelin-Kraut Handbüch, 3 427 (1897)

63. S.Stevanovic, Z. für Kristallographie, 40 321 (1905)

64. R.Ruer & F.Goerens, Ferrum 14 49 (1916)

65. F.Wever, Zeit. anorg. allgem. Chem. 154 294 (1926)

66. R.Ruer & J.Kuschmann, ibid 153 260 (1926)

67. C.H.Desch, Metallography (Longsman-Green) 5th Ed. 1942, p.59.

68. C.O.Bannister & W.D.Jones, Jour. Iron Steel Inst. 124ii, 71 (1931)

69. C.B.Skinner, Cominco Fellow, 1947-48.

70. W.Fehse, Zeit. f. tech. Physik 8 119 (1927)

71. A.T.Larson, W.L.Newton, & W.Hawkins, Chem. Met. Eng. 26 493 (1922)

72. A.Christensen, Zeit. f. anal. Chem. 44 535 (1905)

73. J.W.Mellor, A Comprehensive Treatise on Inorganic and Theoretical Chemistry (Longsman-Green) Vol.VII (1927) p.327

74. I.M.Kolthoff & E.B.Sandell, Textbook of Quantitative Inorganic Analysis (MacMillan) Revised Ed. 1946, p.494.

75. J.W.Mellor, Loc. cit. p.328.

76. Symposium, Temperature - Its Measurement and Control In Science and Industry, Amer. Inst. Physics (Rheinhold) 1941, p.1294-95.

77. M.Benedict, R.S.I. 8 252 (1937)

78. C.E.Waring & G.Robison, R.S.I. 14 143 (1943)

79. R.N.Zabel & R.R.Hancox, R.S.I. 5 28 (1934)

80. W.H.Eccles & F.W.Jordan, Radio Rev. 1 143 (1919)

81. H.J.Reich, Theory & Application of Electron Tubes (McGraw-Hill) 1st Ed. 1939 p.206.

82. J.Millman & S.Seely, Electronics (McGraw-Hill) 1st Ed. 1941 p.334.

83. A.L.Day, R.B.Sossman, & J.C.Hostetter, Amer. J. Sci. 37 1 (1914)